Università degli Studi di Firenze

Dipartimento di Patologia e Oncologia Sperimentali

Scuola di Dottorato di Ricerca in Oncologia Sperimentale e Clinica

XXII ciclo

(MED/04)

Tesi di Dottorato di Ricerca

Metabolic studies on the recruitment into the mitotic cycle of tumour stem cells adapted to hypoxia

Candidato: Dr.ssa Theodora Stivarou

Coordinatore del Dottorato:
Prof. Massimo Olivotto

Tutor:
Prof. Massimo Olivotto

18 Dicembre 2009

INDEX

ABBREVIATIONS

10-HCO-THF	N^{10}-formyl-tetrahydrofolate
BCR	Breakpoint Cluster Region
CH_2-FH_4	N^5,N^{10}-methylene-tetrahydrofolate
CH-FH_4	N^5,N^{10}-methenyl-tetrahydrofolate
cLI(C)	Labelling Index Continuous
cLI(P)	Labelling Index Pulsating
CML	Chronic Myeloid Leukaemia
CSC	Cancer Stem Cells
Cyt	Cytochrome
DNP	2,4-dinitrophenol
DPM	Disintegrations Per Minute
dTMP	deoxythymidine-5'-monophosphate
dUMP	deoxyuridine-5'-monophosphate
F	Folic Acid
FGAR	Formylglycinamide Ribonucleotide
FH_2	dihydrofolic acid
FH_4	tetrahydrofolic acid
FP	Flavoproteins
GAR	Glycinamide Ribonucleotide
GARFT	Glycinamide Ribonucleotide Formyltransferase
H	Hypoxia
HEPES	N-2-hydroxyethylpiperazine-N'-2-ethane sulfonic acid

HPLC	High Performance Liquid Chromatography
HSC	Haematopoietic Stem Cells
IC$_{50}$	Half Maximal Inhibitory Concentration
LI	Labelling Index
PDC	Pyruvate Dehydrogenase Complex
Ph Chromosome	Philadelphia Chromosome
R	DPM x 90 minutes per flask
RT	Room Temperature
S.E.M	Standard Error of Mean
SC	Stem Cells
TCA	Tricarboxylic Acid
TDX	Raltitrexed-Tomudex
TS	Thymidilate Synthase

INTRODUCTION

Stem Cells

In multicellular organisms, cell populations derive from progenitors organized in a hierarchical fashion, with the staminal compartment residing at the apex of developmental pathway (Jordan *et al.*, 2006).

Stem cells are defined as cells endowed with the potential to proliferate extensively, sometimes limitlessly, and with the capacity of self-renewal whereby at least one daughter retains the staminality properties (Mittal *et al.*, 2009). Stem cells not only renew themselves, but also give rise to specialized cell types (Lemoli *et al.*, 2005). As a matter of fact, stem cells can divide symmetrically, whereby each daughter cell retains the properties of the parental cells, or asymmetrically, where, in this case, one daughter cell retains the properties of the parental cell, whereas the other daughter begins the process of determination (Sell, 2004).

According to their differentiation potential, stem cells can be divided into three categories: embryonal, germinal and somatic or adult. Embryonal stem cells are derived from the first five or six divisions of the fertilized egg. The progeny of embryonal stem cells are the precursors for all cells of the adult organs. Germinal stem cells in the adult produce eggs and sperm and are responsible for reproduction. Somatic stem or progenitor cells are considered more limited in their potential, and they produce cells that differentiate into mature functioning cells that are responsible for normal tissue renewal (Sell, 2004). The fertilized egg is defined as a totipotent stem cell, because it can give rise to all cells and tissues of the developing embryo. The embryonal stem cells, which give rise to cells originating from all three germ layers (mesoderm, endoderm and ectoderm), are defined as pluripotent. The latter

proliferate extensively in the embryo, are capable of differentiating into all adult tissues, and can be isolated and grown *ex vivo*, where they continue to replicate and differentiate. Human pluripotent stem cells were found in culture to possess an active telomerase, thus being entitled to replicate for many generations.

Adult stem cells have long-term self-renewal capacity and give rise to mature cell types with specialized functions. Typically, stem cells generate intermediate cell types (progenitors and more differentiated precursors) before they achieve their fully differentiated state. Progenitors and precursors cells are actually regarded as *committed* to differentiate along a specific cellular pathway. So, by definition, adult stem cells should be capable of self-renewal for the lifetime of the organism and of giving rise to fully differentiated cells with mature phenotypes, fully integrating into the tissues, capable of specialized functions (Lemoli *et al.*, 2005).

Cancer Stem Cells

Advances in the field of stem cell biology provided renewed hopes that stem cells can be used to treat a wide range of genetic diseases and traumatic injuries. At the same time, it has been proposed that within the tumor bulk a minor subpopulation play the role of cancer stem cells (CSC). Indeed, recent studies on cancer self-renewal demonstrated that this subpopulation really exists, endowed with an unlimited capacity for self-renewal, together with sufficient plasticity to generate multiform progenies committed to different terminal fates. These committed compartments constitute the highly mitogenic bulk of tumours, that is the real target of conventional antiblastic treatments, whereas the staminal elements survive and prepare relapses (Pardal *et al.,* 2003; Jones *et al.*, 2004; Olivotto and Dello Sbarba, 2008).

4
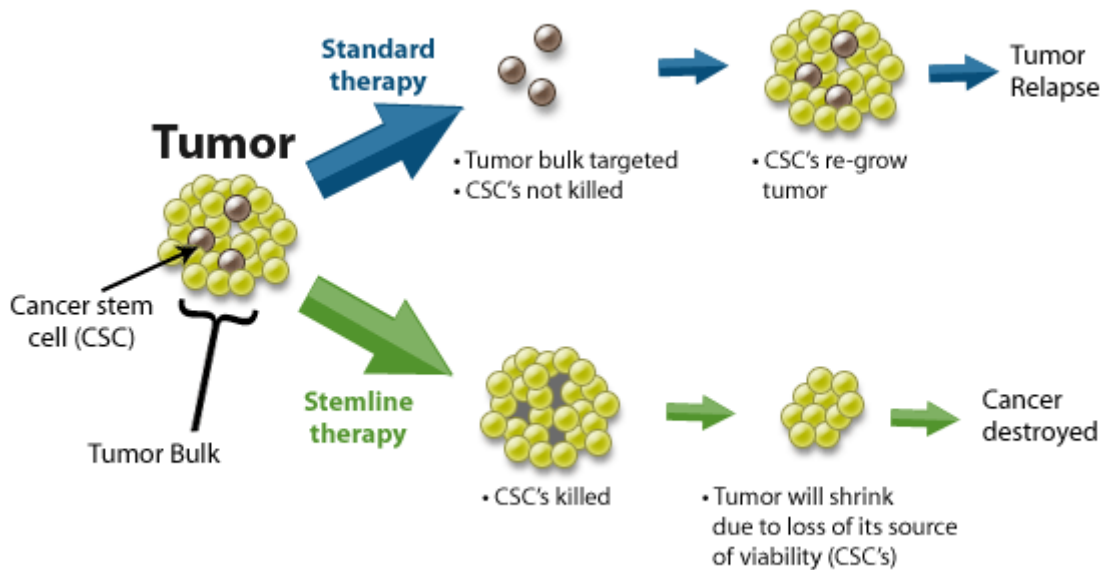
Fig. I. Cancer Stem Cells comprise a unique subpopulation of neoplastic cells within tumours that results to be resistant to standard therapy. Importantly, while conventional anti-cancer treatments (e.g. chemotherapy and radiation) can often transiently shrink tumours by targeting tumour bulk, these therapies fail to target and kill CSCs leading to treatment failure and relapse (Stemline, 2008).

The fact that CSC share some main properties with SC has brought to the conclusion that CSC are the result of genetic and epigenetic mutations in SC, in progenitors or in differentiated cells that re-gain the capacity of self-renewal. As a matter of fact, the very essence of tumor evolution implies that, whatever the hierarchical position of the progenitor targeted by a transforming agent, the neoplastic cell must acquire both the staminal feature of unlimited self-renewal and the genomic instability necessary to modulate its fitness to restricted environments. Actually, CSC can give rise to all the malignant cells of a primary tumor residing in drug-resistant staminal niches responsible for tumour relapses, subsequent a chemotherapy-induced tumor remission, as well as provoking metastases. Moreover, cancer stem cells share with

SC the invasivity and the tendency to migrate as they are able to migrate and proliferate in sites distant from their original sites (Paget, 1889; Fidler, 1978).
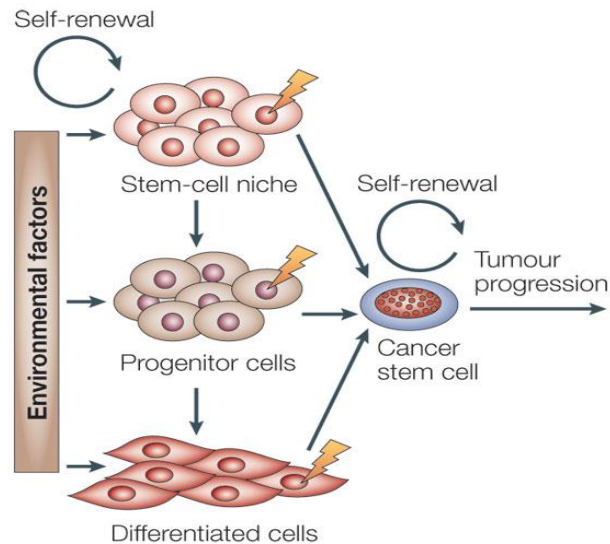
Copyright © 2005 Nature Publishing Group
Nature Reviews | Cancer

Fig. II. Origin of cancer stem cells. CSC may be caused by transforming mutations, derived by numerous microenvironmental factors, occurring in normal stem cells, progenitors cells or differentiated cells (Bjerkvig *et al.*, 2005).

Tumour phenotypes are extremely varying, due to their mixture of differentiated and undifferentiated cells, in the context of abortive attempts to reproduce normal tissues and organs. This variability is further increased by the acquisition of local invasivity and metastatic spread that lead to the progressive loss of differentiation. This evolution was termed by Rous as the "neoplastic progression", to indicate that "cancer changes from bad to worse" (Rous and Beard, 1935).

Nowadays, it is generally agreed that the neoplastic progression is the result of a combination of genetic and epigenetic changes, brought about by mutations and DNA methylation, with a final fate driven by mutagenesis and clonal selection (Klein, 1998; Loeb, 1998; Blagosklonny, 2002). In this light, the term "tumour mutator phenotype" has been introduced to indicate genes that govern any mechanism ensuring genetic stability, such as genes involved in DNA repair and replication as, for example, p53 and DNA polymerase. Alterations of these genes initiate a process which, at each successive round of DNA replication, increases the number of mutations throughout the genome (Loeb and Cheng, 1990).

This progressive increase in cancer mutations is in keeping with the Nowell's definition of cancer as "an evolutionary system, subject to the effects of natural selection, and therefore modulated by the microenvironment" (Nowell, 1976). Actually, this very "Darwinian" account of neoplastic progression leads to interpret tumours as ecosystems exposed throughout their life to environmental challenges (Merlo et *al.*, 2006; Olivotto and Dello Sbarba, 2008).

Tumour Hypoxia

The neoplastic progression implies rapid cellular growth accompanied by the alterations of the microenvironment. To a large extent, these alterations consist in variations of essential nutrients supply, of pO_2 and of pH. These changes are due to the tumour neovascularization process. In order to grow beyond a diameter of approximately 1 mm, newly developing tumors must arrange their own vascular network and blood supply, which they accomplish either by incorporating preexisting host vessels or by forming new microvessels through the influence of tumor angiogenetic factors (Vaupel et *al.*,1989; Fokman, 1990). The newly formed vascular

network differs greatly from that found in normal tissue, typically displaying a broad range of structural and functional abnormalities, including dilatations, incomplete or absent endothelial linings and basement membranes, leakiness, irregular and tortuous architecture, arteriovenous shunts, blind ends, and a lack of contractile wall components and pharmacological/physiological receptors (Vaupel, 2004). These irregularities lead to abnormal and sluggish blood flow, thereby diminishing the delivery of nutrients and O_2 to the tumour cells, with the resultant development of hypoxic or even anoxic areas. These factors that can cause hypoxia are mostly perfusion-, diffusion-, or anemia-related. In particular, perfusion-related anemia is caused by inadequate blood flow in tissues, while diffusion-related (chronic) hypoxia is caused by an increase in diffusion distances with tumour expansion. This causes an inadequate O_2 supply to cells more than 70 µm distant from the nutritive blood vessels. Anemic hypoxia is caused by reduced O_2 transport capacity of the blood subsequent to tumor-associated or therapy induced anemia (Vaupel and Harrison, 2004). In these hypoxic areas, the concentration of glucose is usually very low, prohibitive for normal cell survival, but sufficient to guarantee the CSC to enter a "dormant state".

The Tumour Converging Phenotype

Given that genetic instability is a feature of cancer, one might expect that phenotypic heterogeneity of tumours is destined to increase indefinitely. This assumption seems to be contradicted by the consideration that, if the tumor ecosystem has to evolve a phenotype resistant to mictoenviromental restrictions, this evolution must result in a stable genotype which is fitted to survive internal and external perturbations (Klein, 2003). So, while the changes and variations made possible by the genetic instability of the tumour are practically unlimited, the

microenvironment progressively reduces those possibilities in the struggle for life imposed by hypoxia and nutrient shortage. It would therefore seem that the natural selection of tumours is driven by the need to adapt to a very limited range of microambiental conditions, which in turn implies a substantial convergence in selected phenotypes. Although hypoxia-resistant cells may represent a minority of the tumor population at the beginning of the process, it is only matter of time before the ecosystem is dominated by this final convergent phenotype.

To be "successful" in Darwinian terms, this unique cancer phenotype must include the ability to cope with severe hypoxia and nutrient shortage, a clonogenic capacity, essential to sustain tumorigenicity and a high glycolytic potential, for the production of the necessary ATP amount for survival in anaerobic conditions. Morphologically, these cells must a) present a reduced dimension, b) be dominated by the nucleus to the extent that it will be devoid of any cytological structures exploiting sophisticated functions c) have a scanty endoplasmatic reticulum to minimize protein production at the absolutely indispensable levels d) have an elevated quantity of glucose transporters in order to assume as much as glucose possible from the surrounding hostile environment (Olivotto and Dello Sbarba, 2008).

# Adaptation to Hypoxia of Normal and Neoplastic Hematopoietic Stem Cells

Hematopoietic Stem Cells

The striking adaptation of cancer stem cells to hypoxia is a feature also found in normal Hematopoietic Stem Cells (HSC). In fact, hypoxia is a critical environmental condition for the survival and maintenance of HSC (Cipolleschi *et al.*, 1993).

Actually, bone marrow, the site of postnatal haemopoiesis, is characterized by a marked hypoxia, more than any other adult tissue. This fact, apparently paradoxical owing to the high density of bone marrow microvessels, is explained by the vascular anatomy of the bone marrow tissue. Blood enters the bone marrow space through the nutrient artery, which only branches after penetrating the wall of the surrounding bone, where it originates a microcirculation which anastomoses with that deriving from the periosteal artery. The venous branches from this microcirculation then penetrate into the marrow space to form the sinusoidal network that subdivides the haematopoietic tissue. Therefore, the blood that supplies bone marrow is primarily venous. Moreover, the haemopoietic tissue is made of a thick mass of cells that most of them are in extremely active biosynthetic phases: two factors that increase the competition for the scarce oxygen initially supplied. Consequently, there is a zone, just near to the vessel, in which the cells have at their disposal oxygen and nutrients; this zone borders another one in which cells lack oxygen but not glucose and farther on, a zone lacking both oxygen, glucose and other nutrients. It has been demonstrated that in the first zone the cells are actively recruited into the mitotic cycle, whilst in the third one they die; in the intermediate zone, highly hypoxic but still supplied with nutrients, cells survive indefinitely in a state of complete, but reversible, replicative quiescence, a condition typical of stem cells in the areas devoted to their maintenance, forming the "stem cell niches" (Olivotto *et al.*, 2003).

Biochemical studies (Dello Sbarba *et al.*, 1987) have revealed that haematopoietic progenitors are endowed with an anaerobically-oriented metabolism, essentially relying on glycolysis for energy supply, with minimal oxygen requirement for their maintenance and coordinate expansion.

Thus, "hypoxic niches" in the context of the marrow haematopoietic tissue represent the selective habitat necessary for the maintenance of the stem cell compartment and implies that adaptation to hypoxia is a general feature of stem cells rather than a peculiarity of cancer stem cells (Olivotto *et al.*, 2003). However, normal cells inexorably lose their hypoxia adaptation, among with the other staminality features, once they have migrated out of the original niches, whilst neoplastic cells retain, together with all the other staminality properties, their fitness to survive in hypoxia after their exit from the niche and throughout tumour progression. It seems clear, then, that cancer cells gain an evolutionary advantage by retaining hypoxia adaptation for just as long as it represents an indispensable tool to survive indefinitely in the dormant state, evading antiblastic attacks (Merlo *et al.*, 2006). In other words, a condition which in normal stem cells is no more than a restriction, enabling them to remain in a dormant state, becomes an essential premise of existence in cancer cells, enabling them to survive through alternate aerobic and anaerobic phases in neoplastic progression. This alternating response can be explained by the theory of Quesenberry et al. (Quesenberry *et al.*, 2002) according to which there is no genetically or phenotipically stable stem/progenitor cell hierarchy, but a flexible continuum, where the shift between the stem and progenitor cell phenotypes is reversible, rather than being a uni-directional differentiation step.
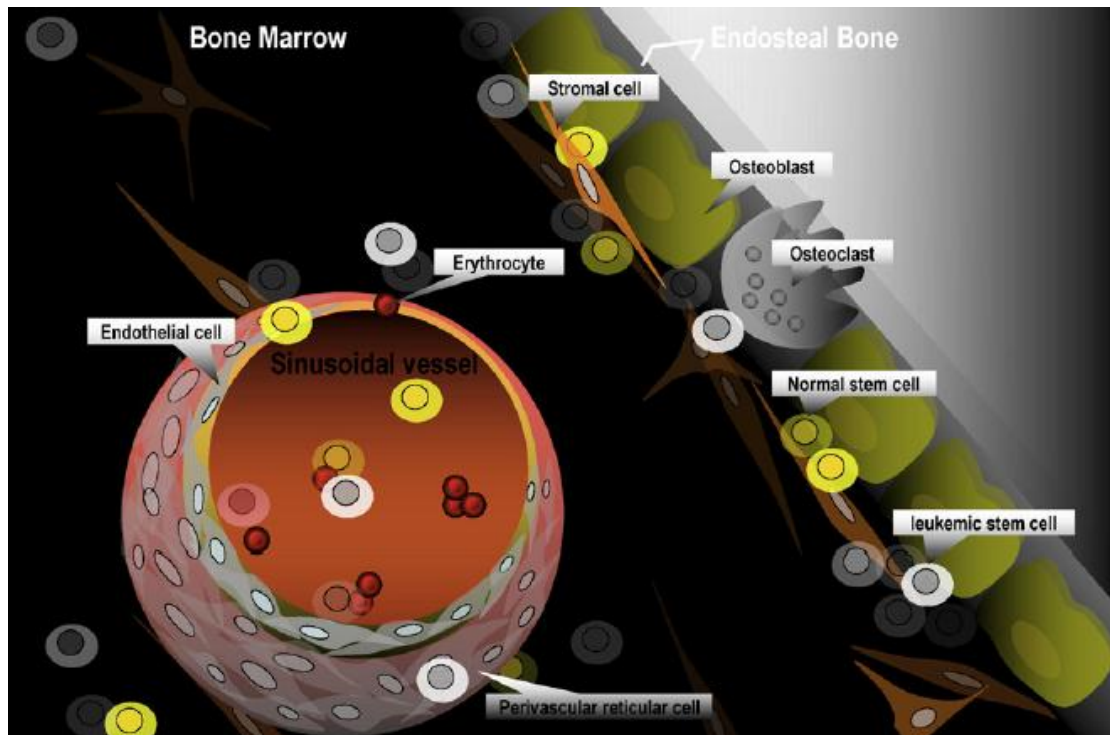
Fig. III. Normal and Leukaemic Stem Cells in the BM microenviroment. In the environs of or at the endosteum, osteoblasts, osteoclasts and stromal cells may provide a quiscent microenvironment for normal and leukemic stem cells. In the vascular niche around sinusoids, perivascular reticular cells, sinusoidal endothelial cells, and mesenchymal progenitors may facilitate transendothelial migration, homing, proliferation and differentiation of normal and leukaemic stem cells (Konopleva *et al.*, 2009).

Leukaemia Stem Cells

The concept of the CSC was first proposed in liquid tumors (myeloma and leukaemia) when experiments showed that only a small percentage (1- 4%) of cancer cells were capable of extensive proliferation and could form colonies (Park *et al.*, 1971; Bruce and Van Der Gaag, 1963; Hamburger and Salmon, 1977; Mittal, 2009). Actually, the demonstration that tumour growth depends on a subpopulation of cancer stem cells in tumours was first described in transmissible leukaemias of mice. Furth and Kahn in 1937 were able to transplant leukaemia from one mouse to another using a single undifferentiated cell (Furth and Kahn, 1937). In 1955, Makino ad Kano obtained clones of tumour cells from single cells (Makino and Kano, 1955).

Human leukaemias manifested gene rearrangements that are present in all the cells of the population, suggesting a tumour origin from a single progenitor cell undergone a malignant gene rearrangement (Rowley, 1999; Schmidt and Przybylski, 2001; Pardal *et al.*, 2003). The effect of a genetic change in the progenitor cell of the population is exemplified by the malignant increase of multiple cell types in chronic mono/myelogenous leukeamias, including various types of polymorphonuclear cells (neutrophils, eosinophils, and basophils), as well as monocytes, erythrocytes and platelets (megakaryocytes), all of which contain the same genetic lesions. In these cases, malignancy can be traced back to pluripotent cells endowed with the capacity to differentiate into multiple types of blood cells (Baird, 2003; Sell, 2004).

Chronic Myeloid Leukaemia (CML) has been one of the first malignancies to which a defined genetic abnormality has been ascribed and is a paradigm for stem cell-derived cancer. Following the post-war atomic testing in the Pacific, increased detection of myeloid leukaemias such as CML was noted among witnesses to those tests. However, little was actually known about the initiating oncogenic event that gave rise to CML, other than that the aberration must arise in an immature HSC, which has the potential to produce many daughter cells as well as identical copies of itself (Jorgensen and Holyoake, 2007). In 1960, Nowel and Hungerford described a shortened chromosome 22 [the so-called Ph (Philadelphia) chromosome] as a consistent chromosomal abnormality associated with a specific type of leukaemia, a breakthrough discovery in cancer biology (Nowell and Hungerford, 1960). It took 13 years before it was appreciated that the Ph chromosome is the result of a t(9;22) reciprocal chromosomal translocation (Rowley, 1973) and again 10 years before the translocation was shown to involve the *abl* proto-oncogene normally situated on chromosome 9 (Bartram *et al.* 1983) and a previously unknown gene on chromosome

22, later termed *bcr* for breakpoint cluster region (Groffen *et al.*, 1984). This novel fusion oncogene created on chromosome 22, and called *BCR-ABL,* (Rowley, 1973) encodes a constitutively active tyrosine kinase of the same name (BCR-ABL), which has proven to be causative of CML, and is nowadays recognized as the target of therapeutic prevention (Sawyers, 1999; Jorgensen and Holyoake, 2007; Deininger *et al.*, 2000).
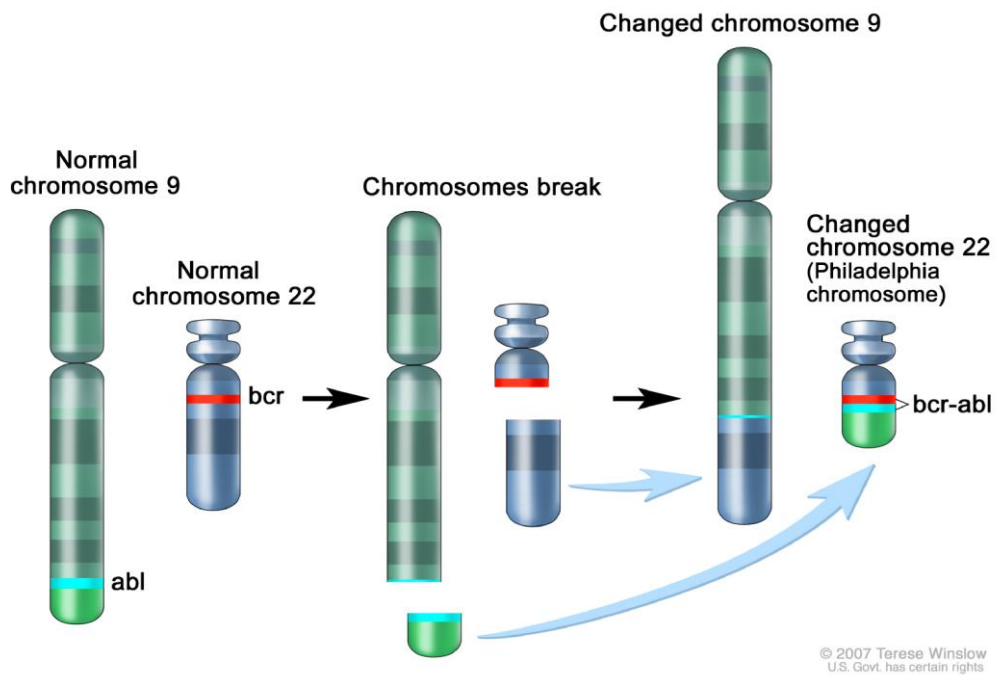
Fig. IV. Translocation (9;22)(q34;q31). On the left; normal chromosomes 9 and 22; on the right chromosome Philadelphia and the derivative chromosome 9 (National Cancer Institute, 2008).

CML is a triphasic myeloproliferative disorder normally initiating with a relatively benign chronic phase (CP) in which Ph is the only genetic abnormality. After 5-7 years, the CP transforms into an accelerated phase (AP) characterized by a huge increase in the number of blast cells in the bone marrow and peripheral blood. This phase is relatively short (6-9 months) and terminates in a blast crisis (BC);

lasting 3-6 months, characterized by numerous additional genetic aberrations in Ph+ HSCs, e.g. trisomy 8 or 17 or i(17q) (Mughal and Goldman, 2006; Jorgensen and Holyoake, 2007).

A widely used model of LSC is the K562 cell line, which is derived from a patient affected with CML at the onset of a BC (see below).

The Yoshida AH130 Hepatoma Model as a Prototype of the Tumour Converging Phenotype

A phenotype mirroring the one of cancer stem cells at advanced stages of neoplastic progression is expressed by experimental tumours which were widely used before the advent of cell culture in vitro, such as the AH130 ascites hepatoma and similar neoplasias. In 1932, Yoshida produced the AH130 hepatoma by treating rats with the potent cancerogen *o*-aminoazotoluene (Yoshida, 1934). He eventually obtained a transplantable, liquid tumour developing in the ascites fluid which is secreted by the vessels of the peritoneal cavity. At the end of its development this tumour contains myriads of isolated cells, a high nucleus/cytoplasm ratio, scanty endoplasmic reticulum and very few mitochondria. On the whole, they appear extremely simplified and devoid of any of the phenotypic markers of the parental hepatocytes, including the histocompatibility antigens.

Each Yoshida cell is capable of generating myriads of identical cells, behaving like stem cells endowed with an unlimited capacity of self-renewal. In fact, soon after transplantation into a new host, the population undergoes an intense proliferation, drawing nutrients and oxygen from the plasma-like fluid exuded from peritoneal vessels. This ability to proliferate weakens progressively when tumour volume and cell number increase, until oxygen and glucose concentrations in the

fluid fall to zero (usually within 5-6 days after transplantation) (Del Monte, 1967; Del Monte and Rossi, 1963). From this time on, cell growth progressively slows down, and reaches its plateau at day 10-11. At this stage, nearly 100% of cells are still alive but they are randomly dispersed in a long G_1 of the mitotic cycle, owing to their inability to enter the S phase (Olivotto, 1979; Olivotto and Paoletti, 1980). This "hibernation" is possible because, even when extremely crowded, cells can move freely in the ascites fluid, residing randomly in different areas of the tumour bulk, although most of the time they are distant from, and only very rarely close to, the peritoneal vessels. This ceaseless change of the environment represents a potent driving force for selecting clones which are adapted to hypoxia and nutrient shortage, as well as able to resume cell growth with the improvement of external conditions. Taken all together, the features just described are typical of dormant cancer stem cells naturally synchronized in a long G_1 (Olivotto and Dello Sbarba, 2008).

The Role of Glycolysis and Mitochondrial Respiration in Normal and Tumour Stem Cells: The Warburg phenomenon

Warburg used to define as glycolysis the process by which glucose 6-phosphate is transformed into lactic acid. The German biochemist used to distinguish an "anaerobic glycolysis", in which lactate is produced in the absence of oxygen, and an "aerobic glycolysis", in which the production of lactate is accomplished in aerobic conditions. He also observed that the cells of adult differentiated tissues carry out the anaerobic and not the aerobic glycolysis; on the contrary, he claimed that only cancer cells produce lactate in the presence of oxygen (Warburg, 1956; Warburg, 1956; Warburg 1959).

Nowadays, we know that glucose transported inside the cell gets consumed in various metabolic pathways especially in glycolysis, today defined as the conversion of glucose to pyruvate. In aerobic conditions, pyruvate enters the Krebs (tricarboxylic acid-TCA) cycle, where its reducing equivalents get oxidized to H_2O and CO_2 through the mitochondrial respiratory chain. The electron transport to O_2 begins with the reduction of mitochondrial NAD to NADH. In anaerobic conditions, electrons cannot be transported to O_2; thus, pyruvate is reduced to lactate instead of entering the Krebs cycle. The latter is fundamental for the conversion of cytosolic NADH to NAD^+ and for triggering one of the crucial steps of the TCA cycle, the oxidation of glyceraldehyde-3-phosphate to 2,3-biphosphoglycerate. Under these conditions, the conversion of glucose to lactate is the only significant source of energy of the cell and occurs when the mitochondrial task is inhibited or insufficient (Nelson and Cox, 2002).

Studies made in Prof. Olivotto's laboratory have proven the Warburg's scheme right, even though its interpretation needs to be substantially revised. It was shown that AH130 cells transition from the G1 cell cycle phase to the S phase is

blocked in anaerobic conditions, for the existence of a limiting step which depends on respiration but not implicated in ATP production (Olivotto *et al.*, 1984).

In order to identify this step, the effects of the block of the electronic flow to O_2 have been compared to those triggered by the uncoupling of the electronic transfer from ATP production. These experiments were carried out by analyzing the effects of Antimycin A and 2,4-dinitrophenol (DNP) on the respiration-limiting steps mentioned above. Antimycin A is a potent inhibitor of the electron transfer through the respiratory chain, and therefore blocks mitochondrial oxygen consumption and the related ATP synthesis to the same extent as anaerobiosis (N_2 incubation). In this respect, Antimycin A mimics the effect of anaerobiosis (Chance and Williams, 1956). On the other hand, DNP uncouples electron transfer through the respiratory chain from ATP synthesis and thus abolish the latter, while enhancing oxygen consumption (Loomis and Lippmann, 1948; Lardy and Wellmann, 1952). The results of these experiments were that, Antimycin A blocked cell recruitment into S, whereas DNP at concentrations increasing the electron flow to O_2, does not have inhibitory effect on cell cycle. ATP measurements showed that cells treated with Amtimycin A and DNP displayed the same levels of ATP, evidently produced by an enhanced glycolysis (Olivotto and Paoletti, 1981).

These results led to conclude that the G_1-S transition in tumour cells depends tightly on the electron transfer through the respiratory chain but not on its oxidative coupling that generates ATP. In other words, the limiting step for cell cycle recruitment is connected with the oxidation of reducing equivalents throughout the respiratory chain, but it has no connection with the mitochondrial ATP production that can be completely substituted by the increment of glycolysis through the Pasteur effect (Ramaiah, 1974; Olivotto and Paoletti, 1981).

In view of the fact that glycolysis has a crucial role in tumour cells survival, we have explored the role of this sugar in the recruitment of resting AH 130 cells into the cycling state. Glucose consumption resulted proportional to the glucose concentration in the microenvironment so that, when this consumption exceeds the optimal request for cell recruitment, the G1-S transition is impaired. This kind of inhibition is observed particularly in hypoxia-resistant cells because of their augmented capacity for transport in glucose. In these cases, it has been observed that the great part of glucose used for glycolysis (80%) gets converted in lactate instead of being directed to the Krebs cycle, whilst approximately 1% of glucose is used for glycogen synthesis. This cytostatic effect is attributable to the conversion of glucose to pyruvate that constitutes a leading substrate of the Krebs cycle; when pyruvate is produced in excess, the reducing equivalents derived from it saturate the respiratory chain. Thus, the conversion of glucose to lactate in aerobic conditions (the Warburg's aerobic glycolysis), represents a defence mechanism of highly anaplastic tumour cells for disposing of glucose taken up in excess. Therefore, what emerged is a paradoxical role of glucose that, at low concentrations, behaves as a vital nutrient whereas at high concentrations is a potent inhibitor of mitotic cycle. Consequently, the cell cycle arrest, can be achieved in malignant cells either by blocking the respiratory chain or by saturating this chain by an excess of reducing equivalents deriving from oxidizable substrates. This saturation somehow impaired some essential reoxidation of cytosolic reducing equivalents, leading to the enhancement of the NAD(P)H/NAD(P) ratio (Olivotto *et al.*,1983). This enhancement interferes with NAD(P)-dependent processes like purine biosynthesis, an essential pathway required for cell recruitment into growth (see Fig.V). In particular, this complex

synthesis requires the conversion of folic acid into N^{10}-formyl-tetrahydrofolate (HCO-FH_4) that gives two carbonic units to the purine ring.

Two intermediate products are formed: N^5,N^{10}-methylene-tetrahydrofolate (CH_2-FH_4) and N^5,N^{10}-methenyl-tetrahydrofolate (CH-FH_4). CH_2-FH_4 has an important role in both purine and pyrimidine synthesis: as far as purine synthesis it concerns, it must be oxidized to CH-FH_4 through the reduction of $NADP^+$ to $NADPH$. In the other hand, CH_2-FH_4 is the co-factor of thymidylate synthase enzyme (TS) that catalyzes the conversion of deozyuridine-5'-monophosphate (dUMP) to deoxythymidine -5'-monophosphate (dTMP). Therefore, the increment of the NAD(PH)/NADP ratio impairs the conversion of CH_2-FH_4 to CH-FH_4 and hence diminishes the purine synthesis, without affecting the pyrimidine synthesis (Nelson and Cox, 2002).
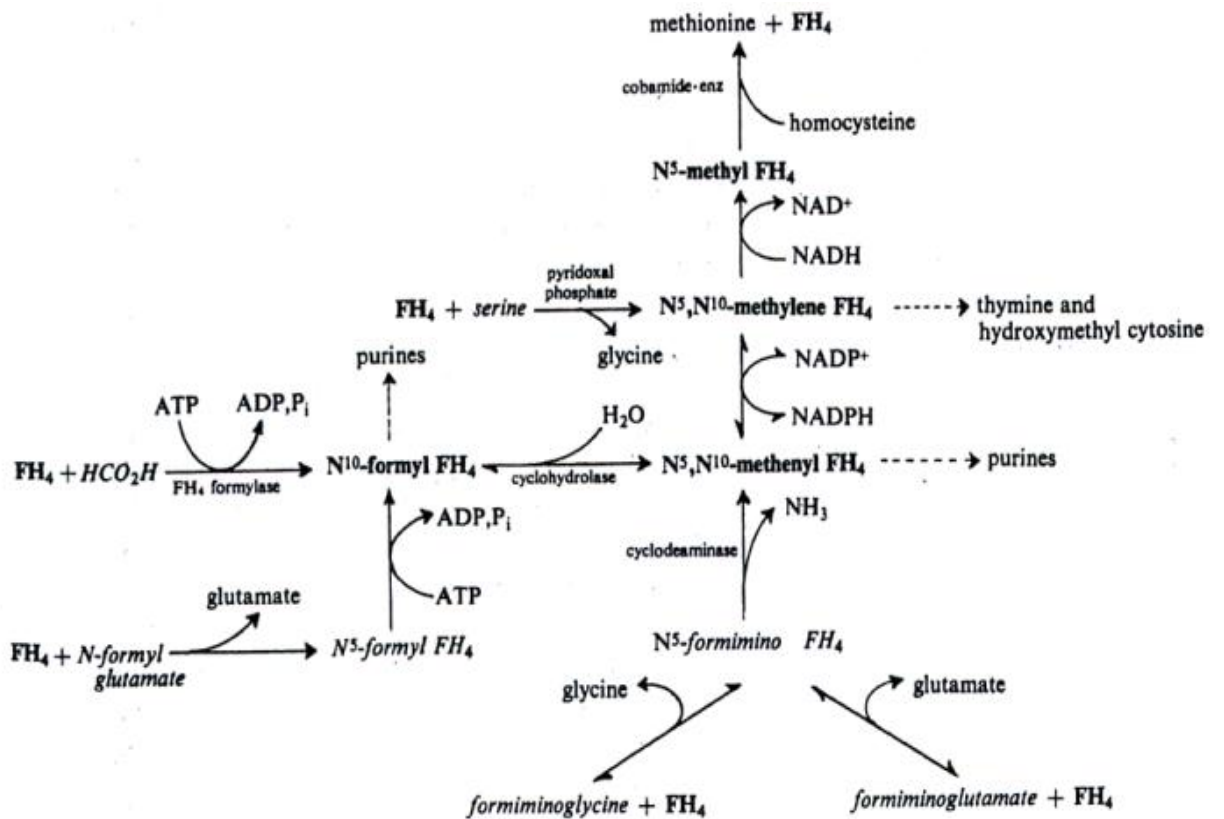

Fig V. Interplay of folates, pyrimidines and purines metabolism.

20

AIM OF THE THESIS

The aim of this thesis has been the definition of the complex metabolic network which controls the adaptation of cancer stem cells to hypoxic microenvironments, and the definition of the fundamental mechanism controlling the transition of the stem cells from the dormant to the cycling state. In particular, we designed to study the role of the mitochondrial respiratory chain and its connection with glycolysis in the regulation of this transition. The revision of the Warburg's theory was also a major task of this work.

MATERIALS AND METHODS

AH130 MODEL

Yoshida ascites hepatoma (AH130) was maintained by weekly intraperitoneal inoculation of 3×10^7 cells in tumour-adapted male Wistar rats weighing 150-200g (Harlan Italy Srl, Correzzana-Milan), given water and food *ad libitum*.

At the time of the experiment (11 days after transplantation), one tumour-bearing animal was decapitated and the tumor was withdrawn by a syringe under sterile conditions. Haemorragic tumors were discarded.

A small aliquot (3 ml) of the tumor was saved; the remainder, usually 70-80 ml, was centrifugated at 6000 RPM for 20 min in room temperature (RT), (Heraeus**®,** Biofuge**®,** Primo R**,** Tabletop Centrifuge), in order to separate the cells from the ascitic plasma, which was collected and used for the preparation of the incubation medium. This ascitic plasma was the only source of exogenous substrates for the cells and had approximately the same composition as the blood plasma (Olivotto and Paoletti, 1974), except that it contained 10-12 mM lactate and no glucose.

Incubation

All procedures were carried out in sterile conditions using sterilized materials. Approximately 1 ml of the ascites fluid was diluted with about 100 ml of medium (see below) to obtain a final concentration of $3-3.5\times10^5$ viable cells per ml.

The medium was prepared by mixing two volumes of the same ascitic plasma in which the cells were grown in vivo (autologous ascitic plasma) with eight volumes of a saline containing 133 mM NaCl; 3.8 mM KCl; 0.58 mM $MgSO_4$; 0.88 mM $CaCl_2$; 0.24 mM Na_2HPO_4; 0.32 mM KH_2PO_4 ; 0.04 mM Phenol red (Fluka, Sigma Aldrich);

antibiotics (100 U penicillin and 100 µg of Streptomycin per ml) (Euroclone). The standard medium (ascitic plasma plus saline) was added with glucose (final concentration 15 mM), buffered with N-2- hydroxyethylpiperazine-N'-2-ethane sulfonic acid (HEPES) (final concentration 20 mM) and adjusted with NaOH at pH 7.6 at room temperature (pH 7.4 at 38° C) (Fluka).

Incubation in normoxia (21% O_2) was carried out in a conventional cell culture incubator in a 5% CO_2, 95% air water-saturated atmosphere.

For the labeling and radioactivity measurements, aliquots of the cell suspension were incubated in air at 38° C in Warburg apparatus (B.Braun, model V85, 80 oscillations per min). Each flask contained 3.0 ml of the cell suspension in the main compartment and 0.1 ml of medium containing the isotopes (see below) in the side arm.

At various intervals after the beginning of the incubation, the isotope solution was tipped into the main compartment of the flasks. At the end of the labeling the contents of the flasks were transferred into a centrifuge tube and spun at 1000g for 10 min. The supernatant was decanted and kept frozen until used for biochemical assays, while the sedimented cells were processed for radioactivity measurements.

Additions

Antimycin A (Sigma-Aldritch) was dissolved in ethanol and added at time zero. The other substrates tested, that is, pyruvate (Sigma-Aldrich); folic, dihydrofolic and tetraidrofolic acid (Sigma-Aldrich); adenine, cytosine (Fluka) and Methotrexate (Sigma-Aldrich, Fluka) were also added at the beginning of the incubation.

Anaerobiosis

To carry out the experiments in anaerobiosis, the saved portion of the tumour was kept in a syringe to avoid any contact with air until zero time. At this point, the amount of the ascites fluid containing the required number of cells was delivered into the main compartment of the Warburg flasks and mixed with incubation mixture, which had been previously and thoroughly flushed with nitrogen. A stick of yellow phosphorus was then put in the central well of the flask, while nitrogen was kept flushing for another 5 min to complete air replacement.

Labeling and radioactivity measurements

The standard procedure for labeling DNA and proteins was a pulse labeling of 90 min at different times from the beginning of incubation. The amounts of the thymidine and lysine incorporated into the trichloroacetic acid (TCA)-precipitable material were measured by labeling the cells with an isotope mixture containing 0.6 µCi of [2-^{14}C] thymidine (T.R.C., Amersham, U.K., 250 mCi/mmole).

10 ml of 10% TCA were added to the cell pellet soon after its separation from the supernatant. The TCA-precipitated material was washed three times, each time with 10 ml of 10% TCA, then dissolved in 0.5 ml of NCS solubilizer (Amersham/Searle Corp.) and counted in a toluene-based scintillation mixture (4.0 g of 2.5-diphenyloxazolone and 0.05 g of 2.2'-p-phenylen-bis-5-phenyloxazolone and 0.05 g

of 2.2'-p-phenylen-bis-5-phenyloxazolone in 1 l of toluene), using a Packard Tricarb 460 CD, set at the dual isotope counting.

Autoradiography

For autoradiographical analysis two types of labeling experiments were performed. In the first, the cells were pulse-labeled for 90 min with 5 μCi of methyl-[^{3}H]thymidine (spec. act. 21 Ci/mmol, T.R.C., Amersham) in order to measure the percentage of cells synthesizing DNA at the various times of incubation; i.e., labeling index pulse = LI(P). In the second type of experiment, the cells were exposed to continuous labeling with 5 μCi of tritiated thymidine from time $t = 0$ until the end of incubation. From these experiments data were obtained on the percentage of cells which had entered into S phase since the beginning of the incubation; i.e., labeling index continuous = LI (C).

Each cell pellet was first washed in 1 ml of cold medium and then fixed by resuspension in 10 ml of acetic acid: methanol (1 : 3) mixture. Subsequently, the fixed cells were washed three times with the same mixture, then concentrated by mild centrifugation and finally spread onto glass slides pretreated with a solution containing 0.05% KCr(SO$_4$) and 0.5% gelatine. After drying of the preparation these were dipped into Kodak NTB-2 emulsion and kept in the dark at 4°C for 20-30 days. After this period the slides were developed for 5 min at room temperature in D-19 (Kodak Ltd.), fixed for 15 min in Kodak fixer and stained with Giemsa.

Assays

Metabolites dosages were carried out on the supernatant of cell cultures by the following enzymatic methods:

Glucose: the dosage measurement was carried out according to the enzymatic method of Werner *et al* (Werner *et al*., 1970).

Lactate: the dosage measurement was carried out according to the enzymatic method of Hohorst (Hoohorst, 1963).

Pyruvate: the dosage measurement was carried out according to the enzymatic method of Bucher *et al.* (Bucher *et al.*, 1963).

HPLC (High Performance Liquid Chromatography) method

Cell organic extraction protocol

1. organic extraction solution: acetonitrile (ultrapure for HPLC) + 10mM KH$_2$PO$_4$ at pH 7.40 (in a 3:1 ratio alias 75% acetonitrile + 25% 10 mM KH$_2$PO$_4$ at pH 7.40).

2. this solution must be insufflated with N$_2$ for at least 20 min before it's utilized and kept afterwards at 4° C.

3. centrifugate the cells (10 millions), remove the supernatant and add 2ml precipitant solution.

4. vortex for about 60 sec.

5. centrifugate at 21.00g/10 min at at 4° C.

6. separate supernatant from pellet and conserve supernatant, well-closed, at -20°C.

7. add in the pellet 1ml of the precipitant solution and repeat 4. and 5.

8. mix the supernatant obtained from the second extraction with the supernatant conserved at -20°C.

9. add chloroform (ultrapure, for HPLC) in the 3ml of the final volume obtained from the 2 extractions with the precipitant solution, according to a 3: 1 ratio respect to the final volume of the supernatant. (In this case 6ml of chloroform must be added).

10. agitate vigorously for at least 90 seconds. Remember that this operation is aimed to remove acetonitrile thus, tubes and taps resistant to aggressive solvents (e.g.chloroform) must be used.

11. centrifugate at 18000g/10 min at 4°C.

12. separate carefully the aqueous phase from the underlying organic one.

13. repeat 9. and 12.

14. after this second washing, the remaining aqueous phase (which will be used for the HPLC analysis) results almost completely devoid of acetonitrile and can be conserved at -80°C until the moment of the analysis.

Buffers for the HPLC course

Buffer A: KH_2PO_4 10mM (Fluka) + Methanol 0.125% (Sigma-Aldrich) + Tetrabutylammonium 12 mM (Nova Chimica)-pH 7

Buffer B: KH_2PO_4 100mM (Fluka) + Methanol 30% (Sigma-Aldrich) + Tetrabutylammonium 2.8 mM (Nova Chimica)- pH 5.5

K562 MODEL

K562 cells were cultured in Roswell Park Memorial Institute (RPMI)-1640 medium supplemented with 50 units/ml penicillin, 50μg/ml streptomycin, and 10% fetal bovine serum (all from EuroClone, Paignton, U.K., http://www.euro-clone.net/), and incubated at 37°C in a water-saturated atmosphere containing 5% CO_2 and 95% air (Heraeus® incubator). Experiments were carried out with cells from maintenance culture, at the time of confluence, plated in 24-well dishes (EuroClone) at 30 x 10^3 /ml.

Assays were performed with the parallel incubation of cells in normoxia (21% O_2 and in the standard conditions mentioned above) and strictly hypoxia. Incubation in severe hypoxia (0.1% O_2) was carried out in a Ruskinn Concept 400 anaerobic incubator flushed with a performed gas mixture (0.1% O_2, 5% CO_2, 95% N_2) and water-saturated. This incubator allows easy entry and exit of materials and sample manipulations without compromising the hypoxic environment. In order to obtain the block or the saturation of the mitochondrial respiratory chain, in a different way from the hypoxic incubation, Antimycin A (Sigma-Aldrich) was added at $6x10^{-6}$ M or, respectively, pyruvate (Sigma-Aldrich) at 10 mM at cultures at time zero of the experiments.

Experiments were carried out with the direct addition of several substrates in the cell suspension contained in every well. The substrates utilized, added in various concentrations (see Results and Discussion) are: folic, dihydrofolic and tetraidrofolic acids (Sigma-Aldrich); adenine (Merck); Methotrexate (Sigma-Aldrich); Raltitrexed and LY309887 (kindly supplied by Prof. Mini, Pharmacology Department; Università degli Studi di Firenze; Florence, Italy).

Measures of cell viability

Cell viability under the various conditions was assayed by the trypan blue exclusion test diluting 1:1 the cell suspension with 1% trypan solution (Sigma-Aldrich). The cell suspension was put into a Bürker chamber and the number of vital cells (trypan blue-negative) was then determined by moltiplicating the cell amount in 1 µl (mean of three squares in 1 mm^2 of the camera grid) for 20000.

Flow cytometry analysis

To determine cell cycle distribution, $5x10^5$ cells were centrifugated for 6 min at 1200 rpm. Once pellet was discarded, cells were resuspended in 500 µl of Propidium Iodide (PI) solution (trisodium citrate 0.1% w/v, NP40 0.1% w/v, PI 50 µg/ml) (Merck4Biosciences Italy, Calbiochem, # 537059), incubated for 30 min at 4°C in darkness and subjected to flow cytometry.

Flow cytometry was performed using a FACSCanto flow cytometer (Becton Dickinson, San Josè, USA) equipped with a 488nm Coherent Sapphire Solid State laser. The filter in front of photomultiplier transmits at 585nm and has a bandwidth of 42nm. A minimum of 30,000 events per sample were analyzed. Data were acquired with the software Diva 6.1.2 (Becton Dickinson) and afterward analyzed with the flow cytometry modeling software ModFit LT (Verity Software House).

Cell lysis

Total cell lysates were obtained as follows: Culture plates were placed on ice, cell monolayers rapidly washed 3 times with ice-cold PBS containing 100 mM orthovanadate and cells lysed by scraping in Laemmli buffer (Tris/HCl 62.5 mM, pH

6.8, 10% glycerol, 0.005% blue bromophenol, SDS 2%) and incubating at 95°C for 10 minutes. Lysates were then clarified by centrifugation (20000 g, 10 min, RT).

Western Blotting and Immunoblotting

Protein concentration was determined by the BCA method and 30-60 μg aliquots of each sample were incubated at 95°C for 10 minutes, in the presence of 100 mM 2-mercaptoethanol. Proteins were then separated by SDS-PAGE in 9-15% polyacrylamide gel and transferred onto PVDF membranes (Immobilon, Millipore, n. cat. IPFL00010) by electroblotting. Membranes were incubated (1 hour, RT) in Odyssey Blocking Buffer diluted 1:1 with PBS, and then in the same buffer containing 0,1% tween-20 and a proper dilution of the primary antibody (16-18 hours, 4°C). After extensive washing with PBS/0.1% tween20, membranes were incubated in Odyssey Blocking Buffer diluted 1:1 with PBS containing a proper dilution of Alexa Fluor 680-conjugated secondary antibody (1 hour, 4°C; Invitrogen A21065). After extensive wash specific bands were visualized by infrared imaging (Licor, Odissey). When needed, membrane stripping was performed by incubation (3x10 minutes, 50°C) in a stripping buffer (62,5 mM Tris/HCl, pH 6.7, 2% SDS, 100 mM 2-mercaptoethanol), followed by extensive washing with PBS and 0.1% Tween-20. Antibodies were used following the manufacturer's instructions: mouse α-p53 (DO-1) diluted 1:1000 (Santa Cruz Biotechnology, # sc-126), mouse α-vinculin diluted 1:1000 (Sigma # V9131).

RESULTS

THE AH130 MODEL

The experimental design and cytokinetics

In Fig. 1 are illustrated the cytofluorimetric and cytokinetic analyses of the G_1/S transition of AH 130 cells after their transfer *in vitro* at the 11th day of the tumour development *in vivo*. Upon their transfer to aerobic cultures in the presence of 15 mM glucose, about 80% of cells are in G1 phase and 10% and 12% are in S and G2 respectively (see also Fig.1B). This striking synchronization in G1 is due to the progressive shortage of glucose and to the complete absence of O_2 in the ascites fluid, typical of ascites tumours at the advanced stage of their development (see Introduction). Upon transfer *in vitro*, the cell cycle distribution changed completely within 18-24 hours, with more than 40% of cells accumulating in S and a concomitant fall of G1 cells from 80% to 45%. From this time on, the percentage of cells in S progressively declines, falling to less than 10%, with return of the G1 cells at the initial percentage.
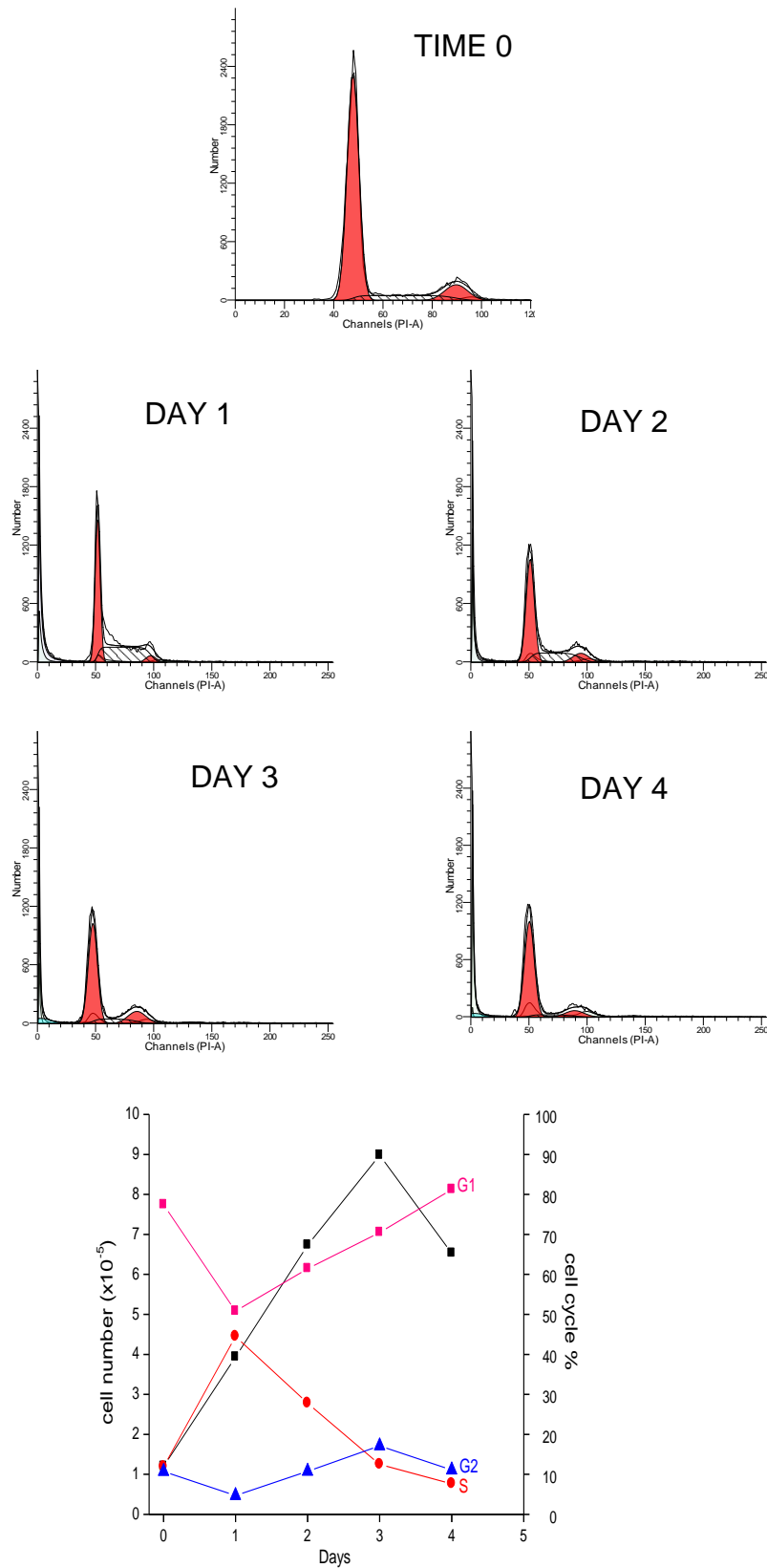
Fig. 1. A. Cell cycle distribution of Yoshida AH130 hepatoma cells during the first 4 days after their transport from *in vivo* to *in vitro*. B. Total number (black) and cell cycle distribution of Yoshida AH130 cells in the various phases as a function of time.

The cytokinetics of the tumour cell recruitment from the non-cycling to the cycling state is also represented in Fig. 2A. In air and in 15 mM glucose (time zero concentration) the cell population, as followed up by the pulse labeling with 14C-thymidine, was recruited into S with a bell-shaped kinetics, whose integration, illustrated by the curve (a), represents the cumulative G1-S transition throughout the experimental time. The percentage of cells recruited into the S phase was determined with: (i) the autoradiographic labeling index procedure, carried out either in pulses or continuous, both corrected for the total cell number (cLI(P) and cLI(C), respectively); (ii) the pulse labeling technique carried out by measuring the rate (R) of ^{14}C thymidine incorporation into DNA according to Olivotto and Paoletti (Olivotto, 1979; Olivotto and Paoletti, 1981). Once corrected for the total cell number in culture, these two techniques proved perfectly consistent. Integrating these pulse measurements throughout the time, it was possible to represent the kinetics of cell recruitment into S, their permanence in and exit from this phase. In fact, a parallel kinetics to the (a) (assigned as curve (b)), shifted by a time corresponding to the length of S (T_S = 15 h), represents the cumulative kinetics of cell exit from S and entry into the G_2/M section of the cell cycle, while cell numbers start to increase after the time T_{G2+M} with the kinetics represented by the curve (b'). The distances from the ordinate axis of the figure to the curve (a) represent the times spent by cells in G_1 before entering the S phase.
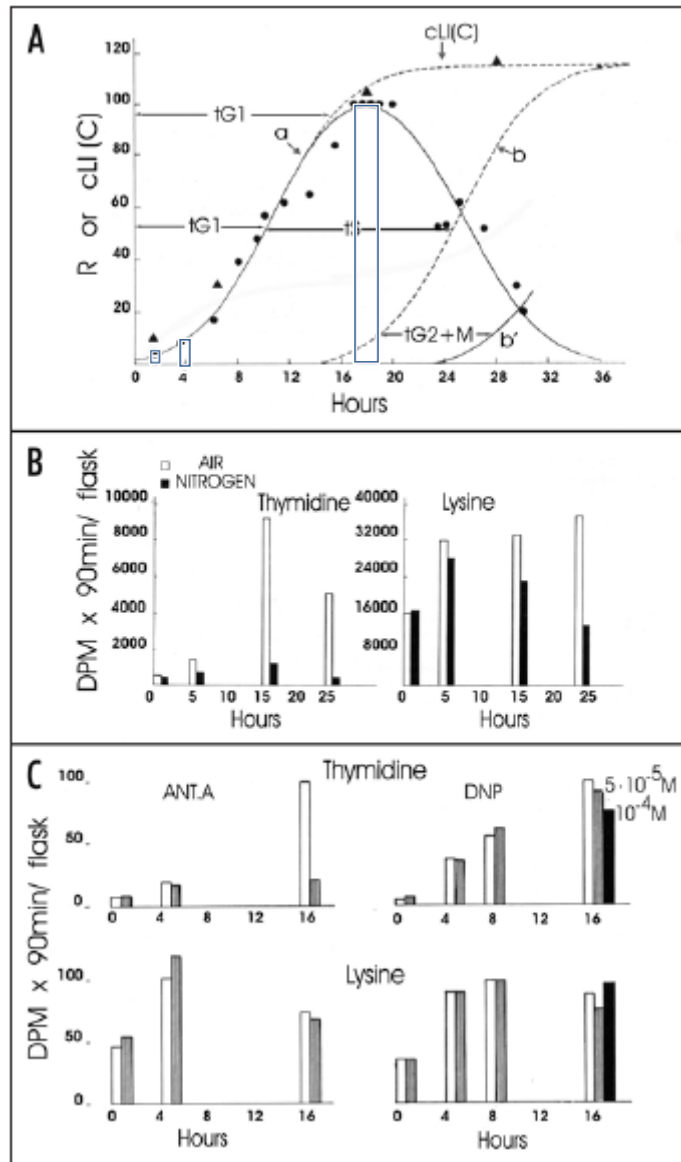
Fig. 2. The tumour cell recruitment from the non-cycling to the cycling state: cytokinetics and respiration-linked limiting step. A. Cytokinetics of cell recruitment. Incubation was carried out in air and with the reconstituted medium added of 15 mM glucose. Circles = rate of ^{14}C-thymidine into DNA (DPM x 90 min per flask = R), expressed as percentages of the maximum value found in each experiment; Triangles = total number of cells entered the S phase since the beginning of incubation, measured by exposing the cells to continuous labeling with ^{3}H-thymidine (Labelling Index Continuous, corrected for the cell increment = cLI(C)). **B.** Time-courses of the rates of ^{14}C-thymidine (left) and ^{3}H-lysine (right) incorporation (DPM x 90 min per flask) in the presence of 15 mM glucose either in air (open bars) or in nitrogen atmosphere (closed bars). **C.** Effects of Antimycin A and DNP on cell recruitment (above) and on the rate of protein synthesis (below). Bars represent the rates of ^{14}C-thymidine or ^{3}H-lysine incorporation (DPM x 90 min per flask) in the absence (open bars) or in the presence (shaded and closed bars) of the inhibitors (3,6 x 10^{-6} Antimycin A; 5 x 10^{-5} and 10^{-4} M DNP). Values are expressed as percentages of the maximum value of the control found in the course of incubation (Olivotto and Dello Sbarba, 2008).

The metabolic features of AH130 cell recruitment into S

Fig. 2(B) illustrates the time courses of the rate of ^{14}C-thymidine (left) and ^{3}H-lysine (right) incorporation in the presence of 15 mM glucose either in air or in nitrogen atmosphere. As shown, cell recruitment into S (estimated by the thymidine incorporation rate (R)) was practically abolished in anaerobiosis (Fig.2B, left), but this did not substantially affect the highly energy-dependent rate of lysine incorporation into cell proteins (Fig.2B, right). These results indicated that the G1-S transition is not limited in anaerobiosis by a significant shortage of ATP which can be supplied by glycolysis. This conclusion was demonstrated definitely by analyzing the effects of Antimycin A and DNP on this process (Fig 2C and Table 1). Actually, the inhibition of the respiratory chain by Antimycin A abolished the cell recruitment, whereas the uncoupling of the oxidative phosphorylation (DNP) did not affect this recruitment.

These effects of the inhibitors were confirmed in our system (table 1A), together with the measurement of intracellular ATP in Antimycin A or DNP-treated cells as in the control (Table 1B).

Table 1

A) Effects of Antimycin A and DNP on the rate of the Oxygen consumption by ascites cells.

	Control	Antimycin A $(3 \times 10^{-6}$ M)	Δ%	DNP $(5 \times 10^{-5}$ M)	Δ%
Rate of O$_2$ consumption (μatoms/min/10^6 cells)	1,99±0,12	0,35±0,10	**-82%**	4,07±0,49	**+104%**

Inhibitors were added at time zero and the O$_2$ consumption was measured with a Clarke electrode at 30°C after 18h of incubation in air at 38°C, in the presence of 15mM glucose. Values are means ± ESM of three separate experiments.

B) ATP levels in ascites cells, measured after 18h of incubation in air or in the presence of Antimycin A or DNP.

	Control	Antimycin A $(3 \times 10^{-6}$ M)	Δ%	DNP $(5 \times 10^{-5}$ M)	Δ%
ATP (μmoles x10^6 cells)	**Exp.1** 15,62±1,33	**Exp.1** 14,17±0,50	**-3%**	**Exp.1** **15,93±0,84**	**-1,8%**
ATP (μmoles x10^6 cells)	**Exp.2** 14,54±0,43	**Exp.2** 13,29±0,45	**-8%**	**Exp.2** 13,69±0,60	**-0,5%**

Values are expressed as μmoles x10^6 viable cells and are means ± ESM of three separate determinations.(Olivotto and Paoletti ,1981).

Moreover, as shown in Table 2, nitrogen-induced anaerobiosis, as well as Antimycin A and DNP, produced the same Pasteur effect, that is, an increase of glycolysis when mitochondrial respiration is impaired. In fact, all three treatments similarly stimulated both glucose consumption and lactate production, which accounted for up to 80% of glucose uptake.

Table 2

The Pasteur effect in ascites cells produced by anaerobiosis, Antimycin A and DNP.

	Control	Antimycin A $(3x10^{-6}$ M)	$\Delta\%$	DNP $(5x10^{-5}$ M)	$\Delta\%$	Anaerobiosis (N_2)	$\Delta\%$
Δ glucose	11,18 ± 0,66 (4)	16,27 ±1,07(4)	**+45%**	15,81 ±0,93(4)	**+41%**	16,94 ±0,80(4)	**+51,7%**
Δ lactate	17,78 ±0,61(4)	30,71 ±1,56(3)	**+72%**	24,13 ±1,93(3)	**+35,7%**	26,60 ±2,21(4)	**+49,6%**

Cells were incubated in the presence of 15mM glucose and values are expressed as μmoles of glucose consumed or lactate produced for 10^6 viable cells, throughout the interval 0-18h and are means ± ESM of a number of experiments listed in parentheses (Olivotto and Paoletti, 1981).

To summarize, the fundamental role played by respiration in tumour cell recruitment into S cannot be attributed to the mitochondrial ATP supply; instead it is conceivably dependent on ATP-uncoupled oxidation through the mitochondrial respiratory chain of reducing equivalents produced in some essential step of cell progression through the cell cycle.

The dependence of cell recruitment into S on glucose supply was object of a complex study carried out previously in our laboratory (Olivotto and Paoletti, 1981). This study showed that the optimal level of recruitment at 18h, indeed required glucose, but the maximum of this parameter was obtained with time zero glucose concentration, at concentrations far lower (0,2-0,5 mM) than those usually used in standard culture media (10-15 mM). Moreover, the above optimal concentrations did not generate any lactate, whereas with 15 mM, up to 80-90% of the sugar was converted to lactate, and the inhibition of this conversion by oxamate drastically reduced the cell recruitment. The negative effect of the high glucose concentration on the G1-S transition was accounted for by the concomitant excess of pyruvate, not converted to lactate and metabolized through the TCA cycle. This conclusion was supported by the experiments reported in Fig.3A, showing the dose-dependent inhibition brought about by pyruvate on cell recruitment into S. A significantly lower degree of inhibition was also produced by others TCA cycle substrates such as oxalacetate and citrate.
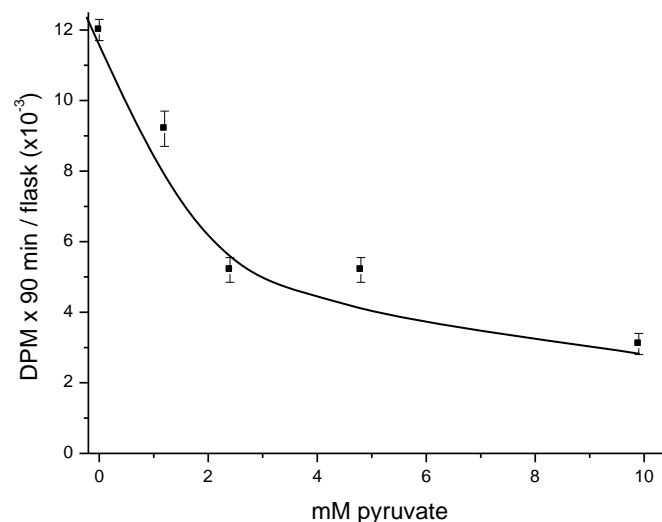
Fig. 3. The Dose-dependence of the cytostatic effect of pyruvate. Values refer to the rate of ^{14}C-thymidine incorporation (R=DPM x 90 min/flask) in air and in the presence of 15 mM glucose (time zero concentration), and are means ± Standard Error of Mean (S.E.M) of three separate experiments. In abscissa are reported the pyruvate concentrations at time zero.

The removal of the inhibition of the G1/S transition

The results presented so far indicated that a respiration-linked step limits the G1-S transition of AH130 cells. This blockage was obtained both by impairing the electron transfer through the respiratory chain (oxygen consumption) by Antimycin A or nitrogen atmosphere, but also by an excess of oxidizable substrates metabolized through the TCA cycle. This suggested the hypothesis that this inhibition depends on the impairment of some redox metabolic step, necessary for cell recruitment to S. Conceivably, this step was attributable to one or more cytosolic NAD(P)-dependent reactions among the multitude of the reactions governed by the cellular redox state. In fact, this kind of reactions should be limited at the end of long incubation periods of impairment or saturation of the respiratory chain. One feasible candidate for this type of metabolic pathways was the NADP-dependent step of folate metabolism implied in the synthesis of the purine ring (see also the Concluding Remarks).

To test this hypothesis, we explored the effects of the addition of folate or pre-formed purine bases to our system in the absence or in the presence of inhibitors of the cell recruitment into S.

As shown in Fig. 4, folate stimulates cell recruitment in air and substantially removes the inhibitory effects of both Antimycin A and pyruvate. Noteworthy, the stimulatory effects of reduced derivatives of folate (FH_2 and FH_4) were significantly lower than those of the oxidated form.

In the same Fig.4, the effects of 0,1 mM adenine are reported. The latter, although displaying slight inhibitory effects on the control, substantially removed the inhibition of Antimycin A and pyruvate. These results indicate that the intracellular pool of adenine is at its optimum for cell recruitment to S in air, but it becomes insufficient in hypoxia.
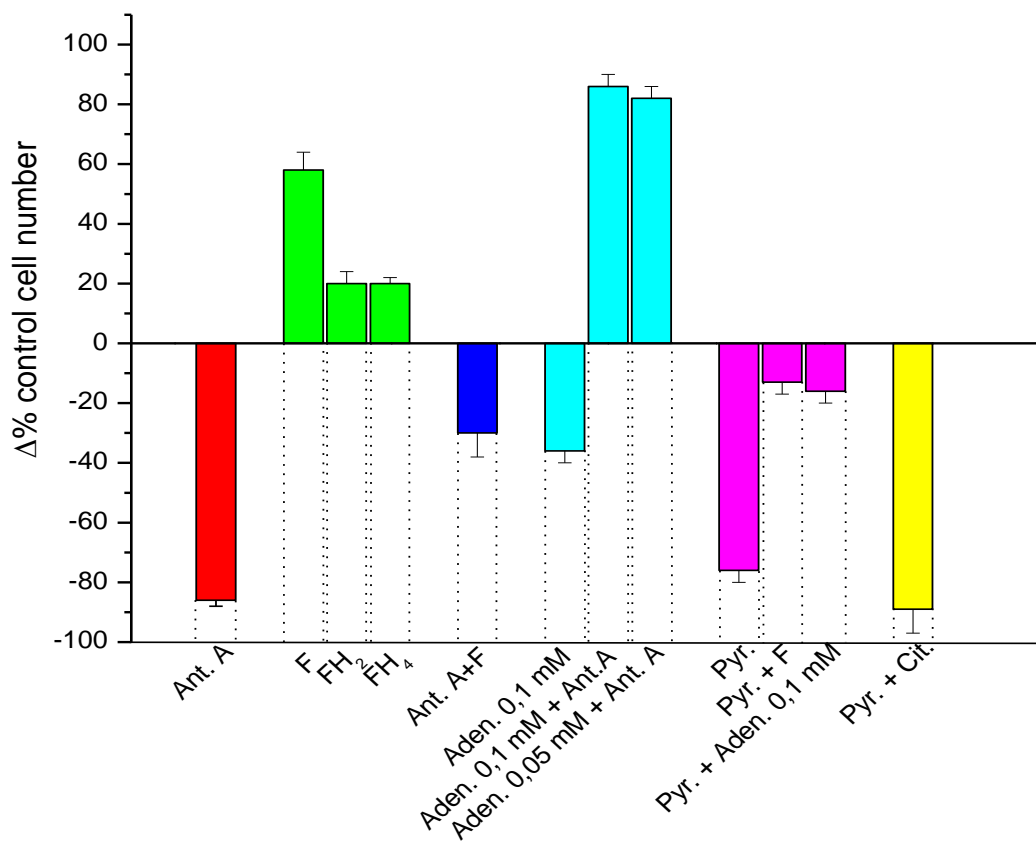
Fig. 4. Effect of folic, dihydrofolic and tetrahydrofolic acids (40μg/ml), adenine and cytosine (2mM) with or without Antimycin A (6 x 10^{-6} M) and pyruvate (10 mM) on the AH130 cell recruitment into S. The values reported here are means ± SEM of three separate experiments.

The dose dependence effects of adenine and pyruvate on our system in air is illustrated in Fig. 5.
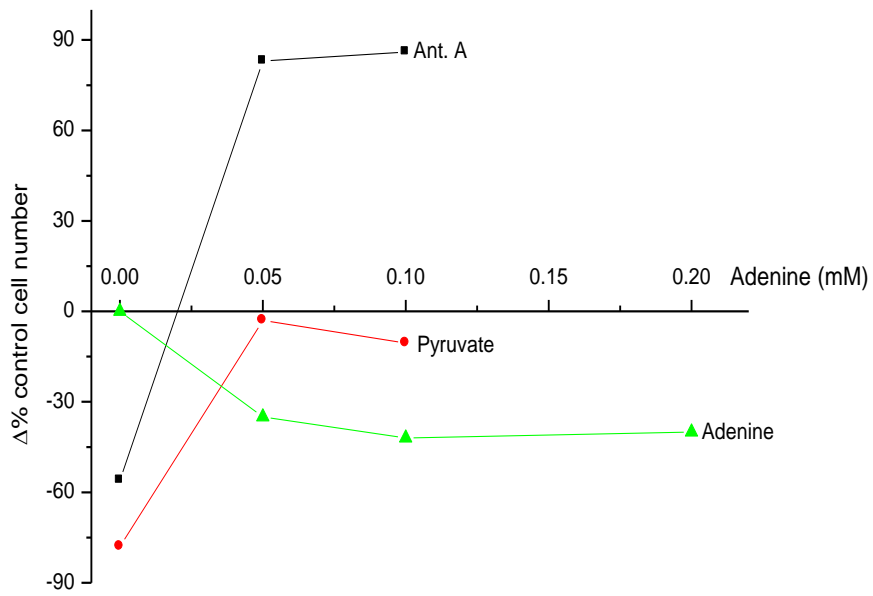
Fig. 5. The dose-dependent removal of the inhibitory effects of Antimycin A 6x10^{-6} M (black) or pyruvate 10 mM M (red) by the addition of adenine 0,1 mM. In green, the adenine effects on controls. Values are means ± SEM of three separate experiments and are expressed as percentages of the respective controls.

A
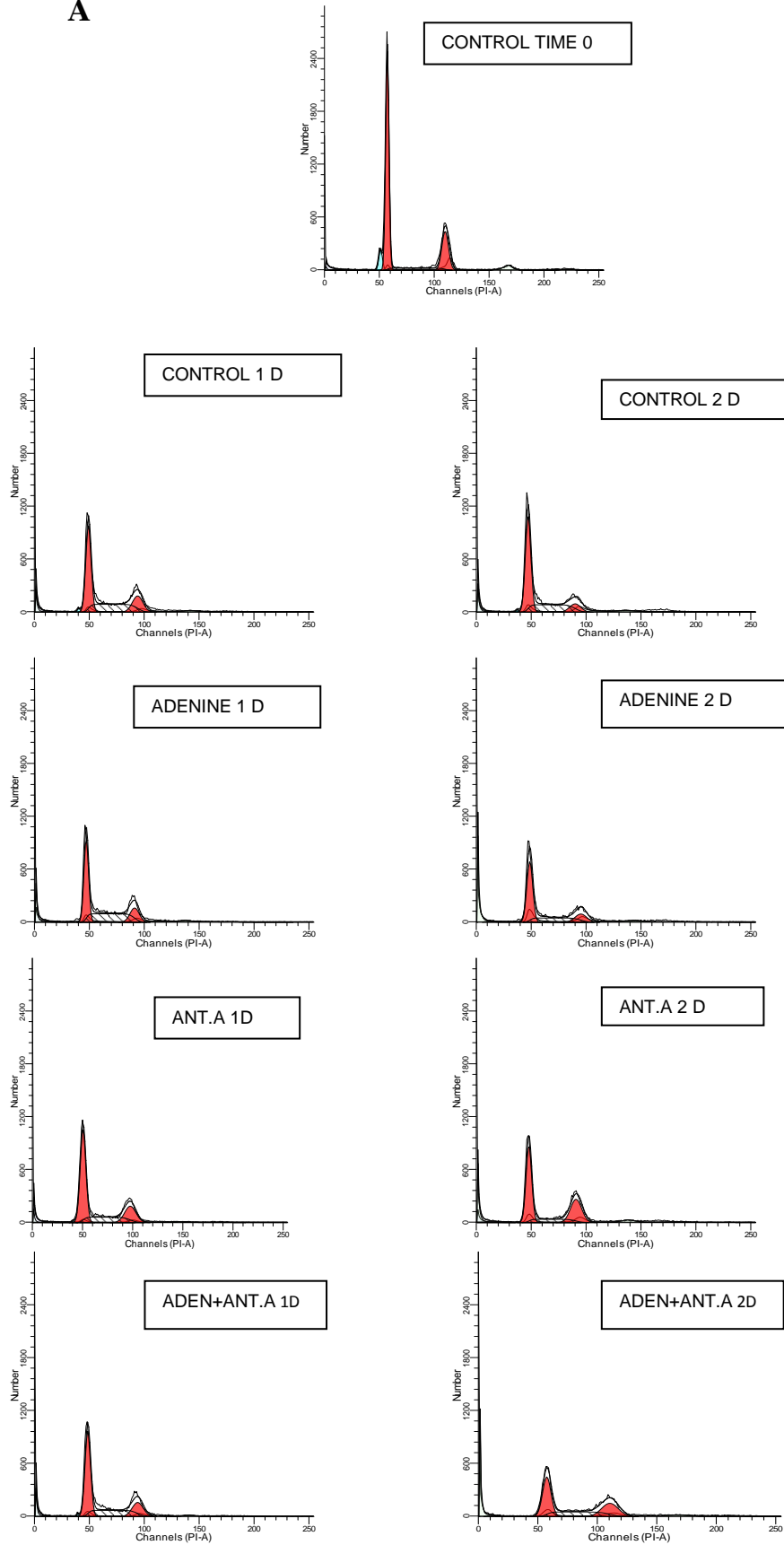
Fig. 6 A. Cell cycle distribution of AH130 cells in Adenine (Aden.) and/or in Antimycin A (Ant.A).

B
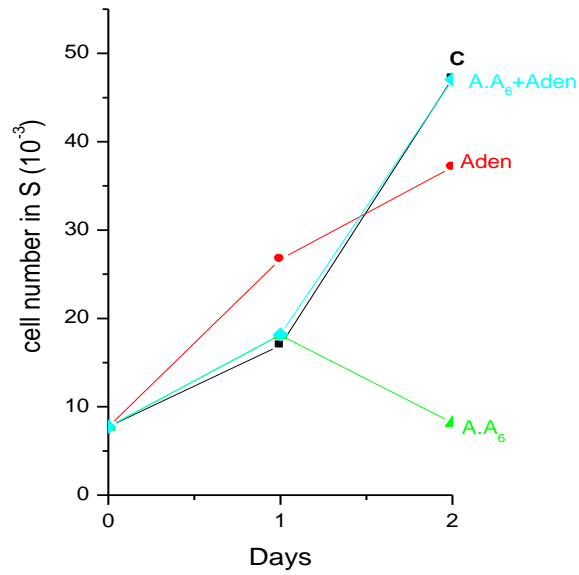
Fig 6 B. The quantititative estimate of the AH130 distribution in S. The experiment conditions were the same as in Fig. 5. A.A = Antimycin A (6×10^{-6} M), Aden.= Adenine (0,1 mM). The number of cells was calculated from the total number of cells scored at various days times for the percentage distribution in S given from A.

The cytofluorimetric analysis of the effects of adenine are also illustrated in Fig.6, where data are reported before and after the correction for the cell viability in S. It is evident that Adenine removes the inhibition of the G1/S transition produced by Antimycin A or pyruvate.

44

THE K562 MODEL

Even though AH130 hepatoma represents the prototype of the convergent profile of highly anaplastic cancer stem cells, we have considered necessary to compare the results provided by this model to those obtained from other types of anaplastic CSC population as farthest as possible from a histogenetic and clinical point of view. To this purpose, we chose the K562 cell line, which represents the extreme anaplastic stage of a CML blast crisis and present all the characteristics of tumour staminality.

The experimental design and cytokinetics

Fig 7A shows the expansion *in vitro* of K562 cells incubated either in the control (normoxia, 10mM glucose) or hypoxic conditions, simulated by N_2 atmosphere or Antimycin A addition. As shown, both these treatments practically abolished the cell expansion, indicating a strict dependence of the cell growth on the activity of the respiratory chain.

The cytofluorimetric analysis of the control cell population during its expansion *in vitro* is reported in Fig. 7B, revealing the typical cell cycle distribution of a fast growing population (35% cells in G1, 53% in S and 12% in G2/M) up to day 4. On the contrary, at the same time, Antimycin A-treated cells appeared substantially accumulated in the S phase, an effect that is much more evident at day 7, when it is accompanied by a marked cell apoptosis.

Thus, from a metabolic point of view, the K562 model responds differently to the blockage of the respiratory chain as compared to the AH130 population, undergoing a blockage in S instead of in G1.
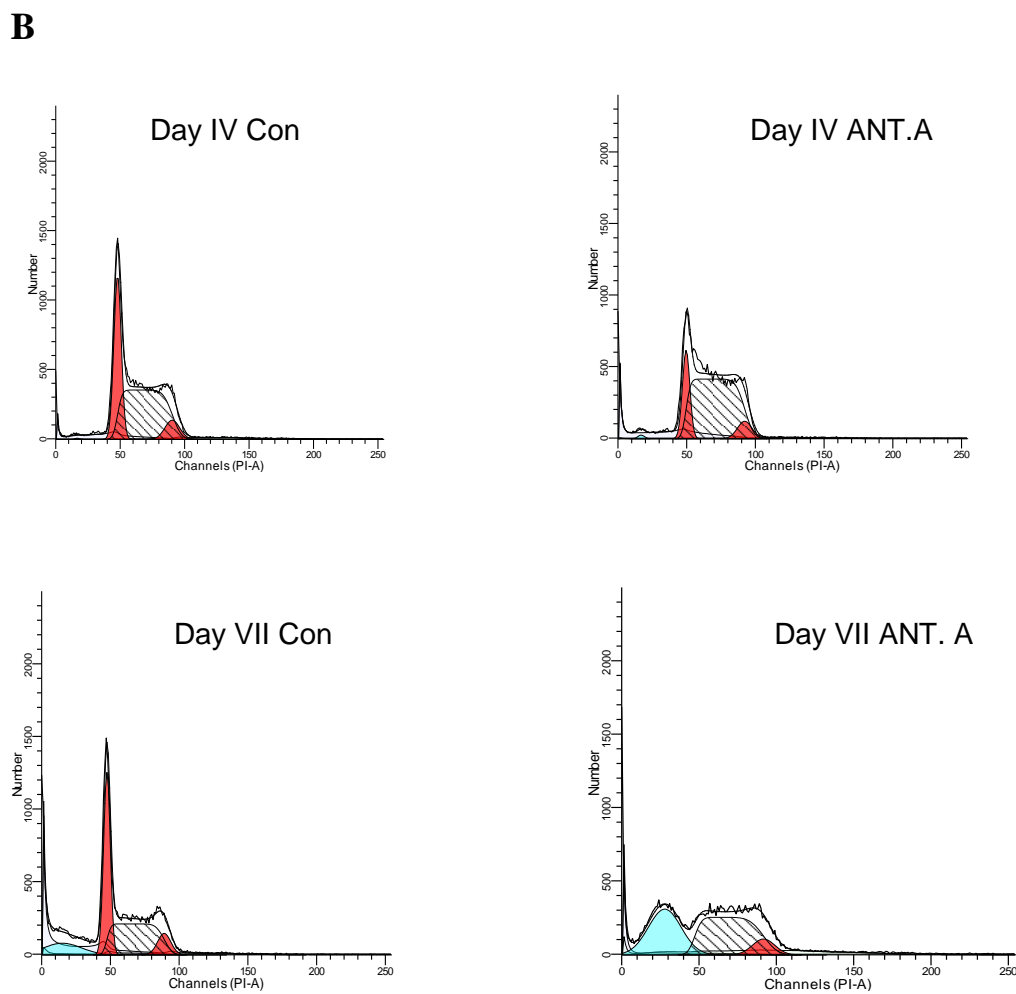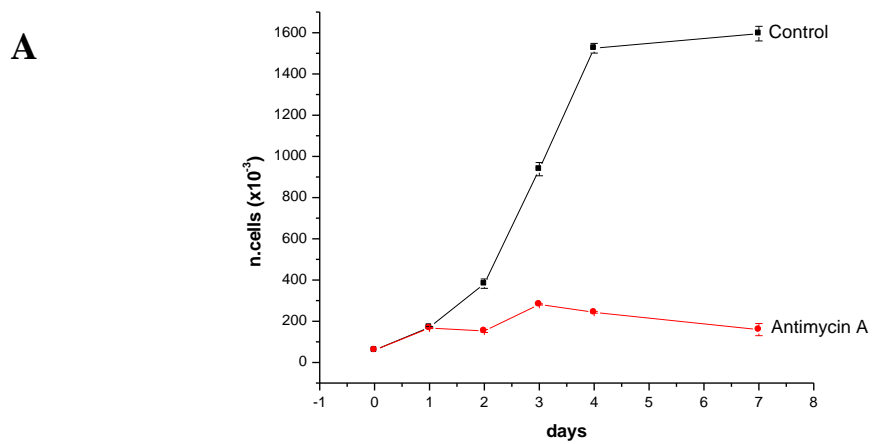
Fig. 7. The K562 proliferation and cytokinetics in normoxia (Con = Control) and in Antimycin A (Ant. A = Antimycin A). The values reported in 7A are means ± SEM of three separate experiments.

To study the capacity of K562 cells to resume growth upon removal from a N_2 atmosphere, we performed the experiment reported in Fig.8, showing that this removal produces a complete recovery of the cell expansion at the same level as that provided by the first seed. These experiments lead us to the conclusion that N_2-incubation selects for a hypoxia-resistant stem cell compartment, entitled to resume the growth kinetics displayed by the control cultured in normoxia, as soon as the hypoxic conditions are removed.
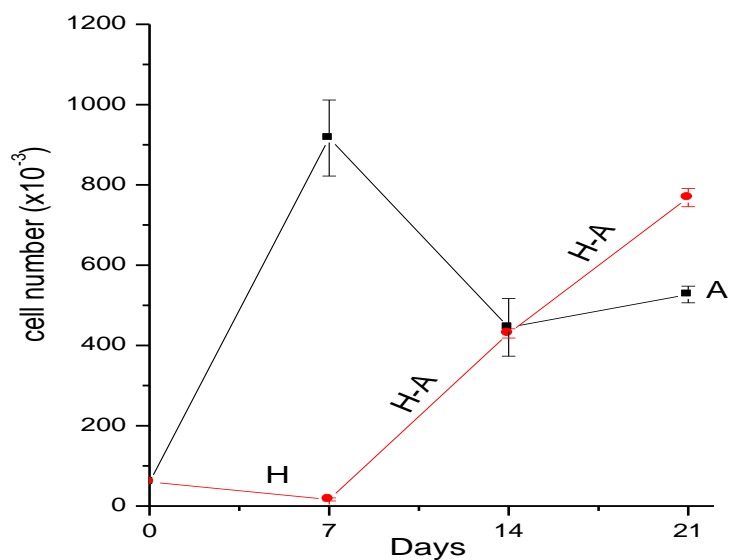
Fig. 8. Time course of K562 cell growth in conditions of normoxia (A-Air), hypoxia (H) and in normoxia after a 7-days N_2-incubation (H-A). The values reported here are means ± SEM of three separate experiments.

From a molecular point of view, the mechanism blocking the mitotic cycle of these two types of cells was further exploited, showing that, both the blockage in G1/S of AH130 cells and in S/G2 of K562 cells is not mediated by p53, which is not expressed in both populations (Fig. 9).
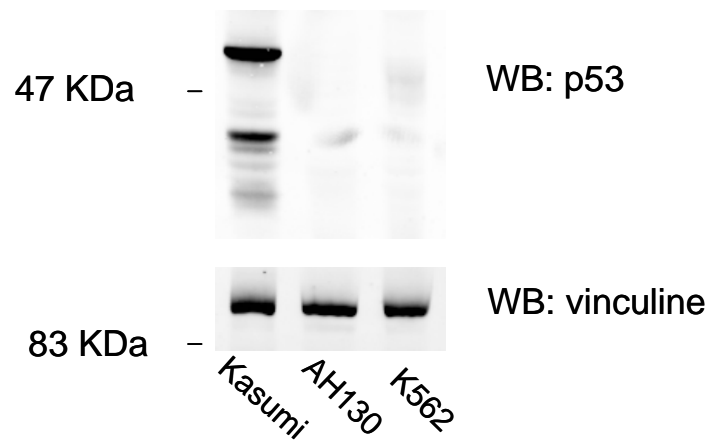
Fig. 9. p53 transcription factor is not expressed either in AH130 cells or in K562 cells. Immunoblot analysis of p53 expression in lysates of AH130 cells, K562 leukaemia cells and Kasumi acute myeloid leukaemia cells-the latter used as a p53 expression control cell line. On the same membrane, vinculine expression was tested as immunoblot control.

The removal of the growth arrest by folate

The experiments reported in Figs 10 and 11 show that, after a 7-days incubation in hypoxia, cells transferred to normoxic conditions display similar growth kinetics in presence or in absence of folate in culture.
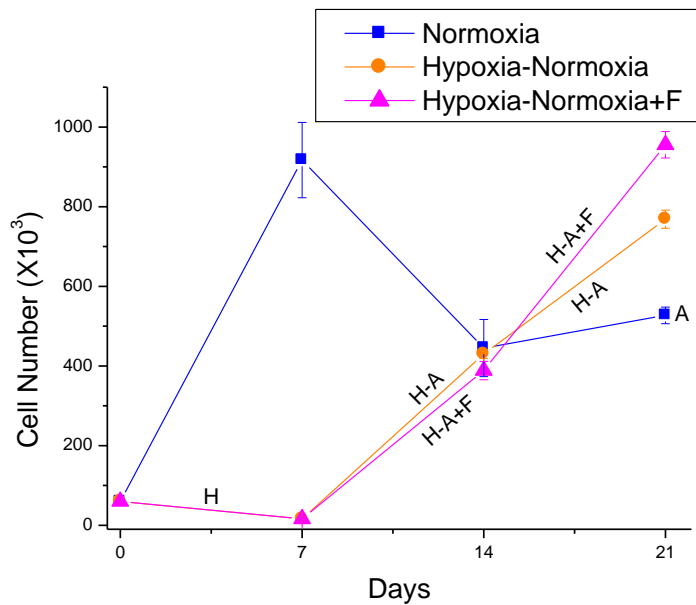
Fig. 10. Time course of the kinetics of K562 cells cultured in a 21-day incubation in normoxia (blue-A=Air), in a 7-day incubation in hypoxia (H=Hypoxia) + 14 days in normoxia with (rose-H-A+F) or without (yellow-H-A) folic acid 40 μg/ml (F=Folate). Values are means ± SEM of three separate experiments.

On the other hand (Fig.11), in N_2 atmosphere, folate determined a substantial expansion of the population, indicating that the growth promoting effect of this vitamin takes place only in hypoxic conditions.
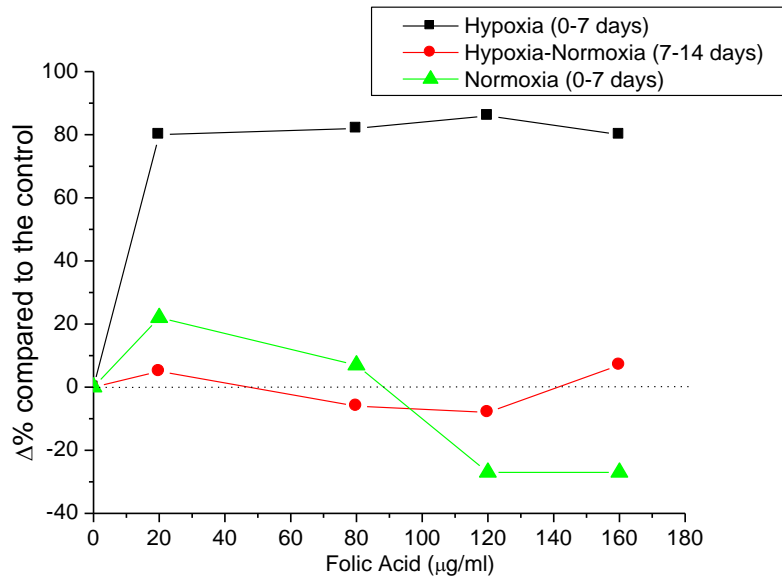
Fig. 11. Dose-dependent effect of acid folic on K562 growth in anaerobic and aerobic conditions. The values reported here are means ± SEM of three independent measurements.

In conclusion, K562 cells share the response to folate displayed by the AH130 cells as far as the removal of the block in hypoxia is concerned. Despite the different position of the blockage within the cell cycle, this similarity seems to imply a similar metabolic nature of the limiting step of cell growth in the two types of cell populations. This in turn led us to hypothesize that the K562 cells undergo a shortage of the purine ring in hypoxia. This hypothesis was tested in the experiments reported below.

The effects of specific inhibitors of the synthesis of purine and pyrimidine bases on K562 cell recruitment into the cycling state

In Fig.12 are shown the effects of typical specific inhibitors of the synthesis of the purine and pyrimidine bases on K562 cells. We used two typical antifolic agents, namely the inhibitor of the synthesis of purines LY309887, and the inhibitor of the pyrimidines synthesis Raltitrexed (brand name Tomudex).

LY309887 is an antimetabolite used for the treatment in colorectal cancer (Assaraf, 2007). It is a specific inhibitor of glycinamide ribonucleotide formyltransferase (GARFT), that blocks the purine *de novo* synthesis and hence produces a depletion of purine nucleotides (Lu et al, 1999). Precisely, this enzyme catalyzes the synthesis of formylglycinamide ribonucleotide (FGAR) by the transport of a formyle group, obtained from 10-HCO-THF, to glycinamide ribonucleotide (GAR).

TDX is a chemotherapeutic agent also used for the treatment in colorectal cancer, since 1998. It is a powerful inhibitor of the thymidilate synthase and hence, of the biosynthesis of the pyrimidine nucleotides precursors (Cunningham, 1998; Botwood 2000; Van Cutsem, 2002).

In Fig. 12 is reported the dose-dependence effects of LY and TDX on K562 cell growth. It is evident that LY (IC_{50} LY309887= 2.5×10^{-9} M) is 1 log more efficient than TDX (IC_{50} TDX= 5×10^{-8} M), suggesting that K562 are much more sensitive to the inhibition of purines than pyrimidines synthesis.
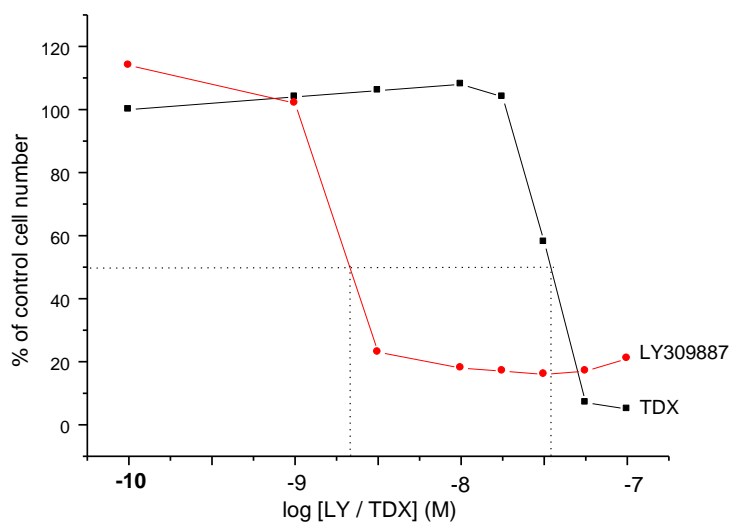
Fig. 12. K562 proliferation following the administration of TDX (black) and LY309887 (red) in the culture. The values reported here are means ± SEM of three independent measurements and are expend as percentage of therapeutic controls.

The specificity of LY309887 activity on purine synthesis was confirmed in the experiments presented in Fig. 13 where it is shown that this agent at 5×10^{-9} M causes an 80% blockage of cell growth in air with a mechanism reversed by the addition of adenine either in air or in Antimycin A.
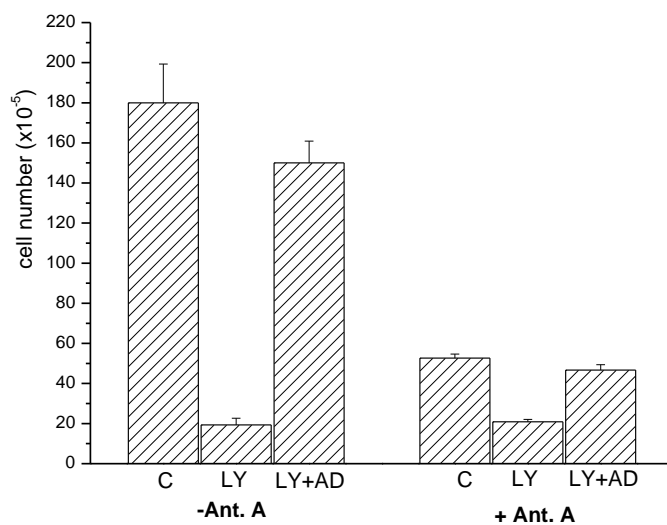
Fig. 13. Influence of LY309887 addition in K562 cultures either in the presence or in the absence of Antimycin A (6×10^{-6} M), with or without the addition of Adenine 0,1 mM. The values are means ± SEM of three independent measurements.

The same applies if one considers the effects of LY309887 in the presence or in the absence of adenine, as explored by the cytofluorimetric analysis reported in Fig. 14. In fact, LY309887 produces a strong cell accumulation in S, similar to that of Antimycin A, an effect totally removed by adenine. These experiments indicate that the Antimycin A blockage of K562 cell growth is related with the impairment of the purine bases synthesis.
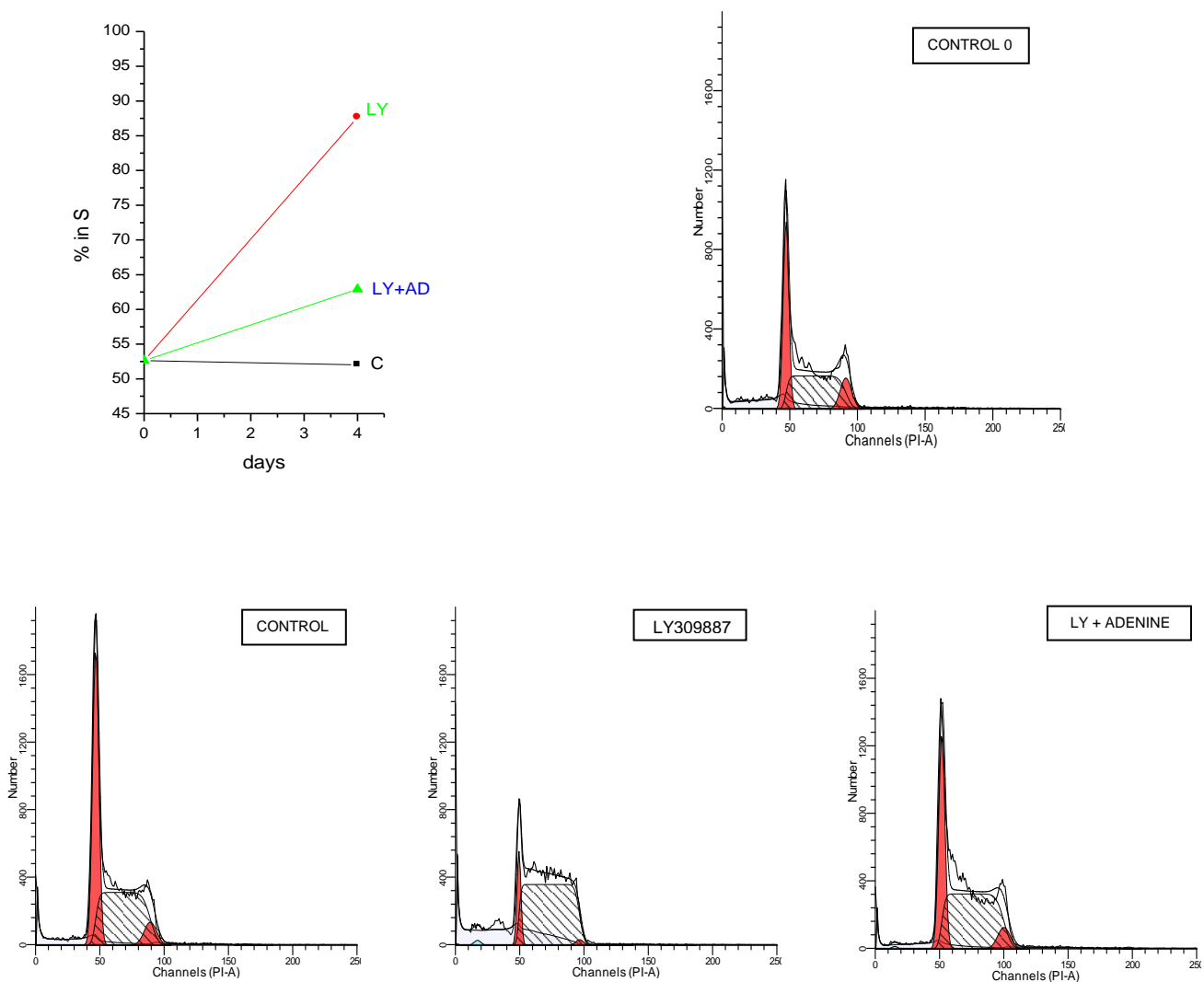
Fig. 14. K562 cells percentage in S phase following to treatment with LY309887 5 x 10^{-9} M in presence or in absence of adenine. Means ± SEM of three independent measurements.

That purines synthesis is a crucial target of treatments blocking or saturating the respiratory chain is further supported by the demonstration that the specific inhibitor TDX, at concentrations up to 10^{-8}, only slightly impairs cell growth in air, while strongly stimulates it in Antimycin A (Fig.15 A and B). This modest inhibition of pyrimidine synthesis, far from inhibiting, promotes K562 cell proliferation.

A

B
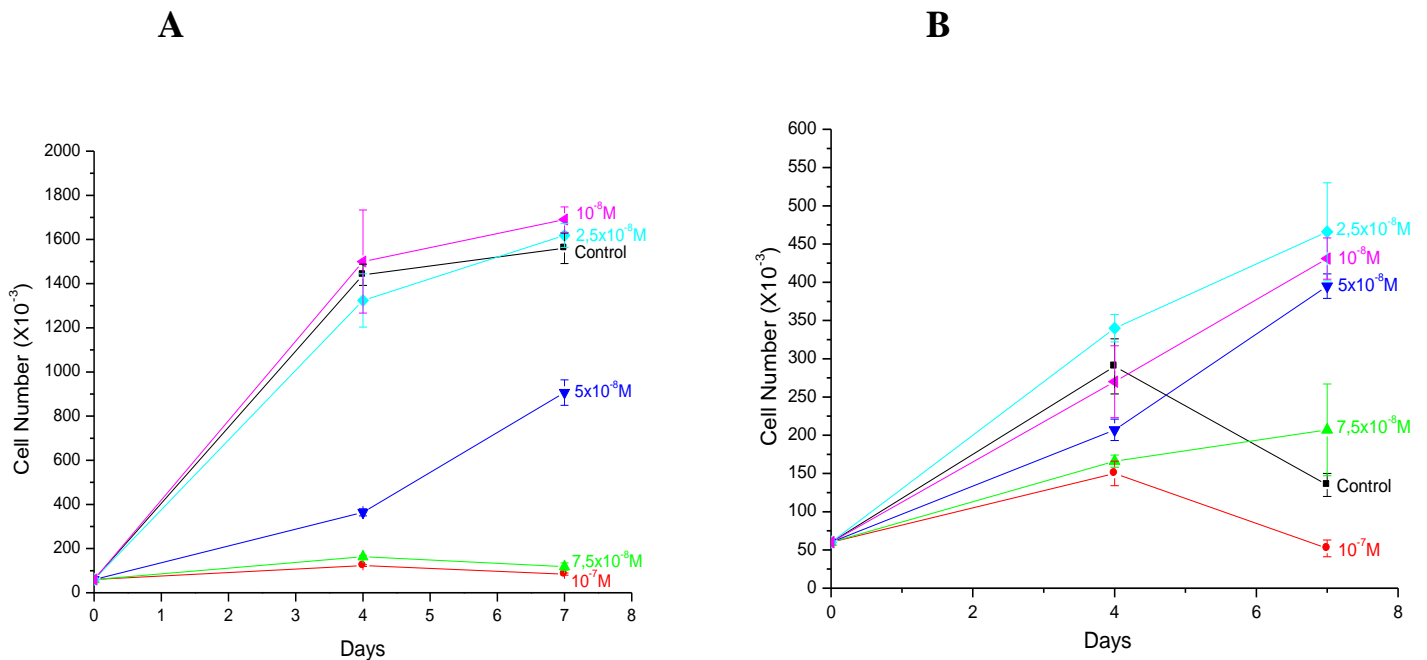
Fig.15 A, B. Dose-dependent influence of TDX on K562 growth in normoxia (A) and in Antimycin-A treated cultures (B). Means ± SEM of three independent experiments.

C
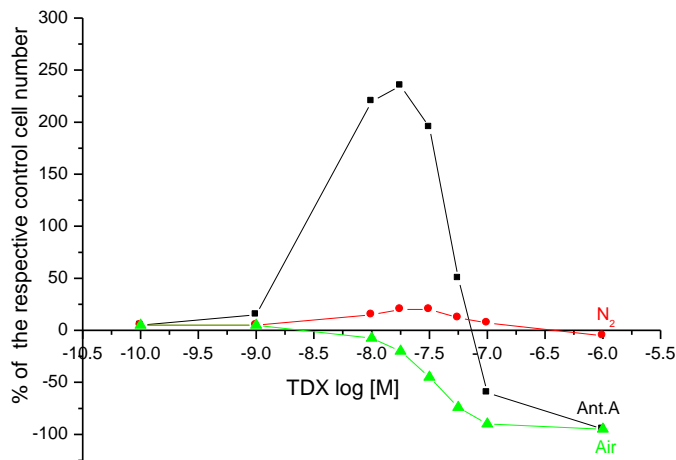
Fig.15 C. K562 growth respect to control cell, in TDX-treated cultures, in aerobic (green) and anaerobic conditions induced by either an N_2 atmosphere (red)or Amtimycin A (black). Values reported means ± SEM of three separate experiments and are expressed as percentage of the respective controls.

The effects of addition of purine and pyrimidine bases on the K562 cells recruitment into the cycling state

Decisive clues to prove the crucial and exclusive role of purine synthesis in the K562 cell recruitment into S were obtained by adding all series of purine and pyrimidine bases in culture. As shown in Fig. 16, while the mixture of all pyrimidine bases (cytosine, thymidine, uracile) tends to further depress the low control rate of recruitment in Antimycin A, the combined addition of adenine and guanine produced a substantial (up to 60%) stimulation in the concentration range of 0.2-0.25 mM. Noteworthy, the single addition of adenine resulted much less efficient, or even

inhibitory, beyond 0,1mM. The single addition of guanine is inhibitory across the whole dose response.

Several relevant implications can be derived from these results: a) the inhibitory effects of pyrimidines and the substantial stimulation by purines point out that cell the recruitment into S of K562 cells is limited by purine shortage, while it is fully sustained at the optimal level of intracellular pyrimidine pool. However, the increase of the purine pool must be contained within a definite threshold, beyond which the recruitment is impaired. The same happens when the single addition of adenine or guanine perturbs the adenine/guanine equilibrium favoring the one or the other.

On the whole, our findings indicate that the K562 recruitment requires a proper equilibrium among the various pools of nucleotide bases, so that the alteration of this equilibrium impairs the growth resumption as far as it generates a shortage of purines without significantly affecting the pyrimidine basis.
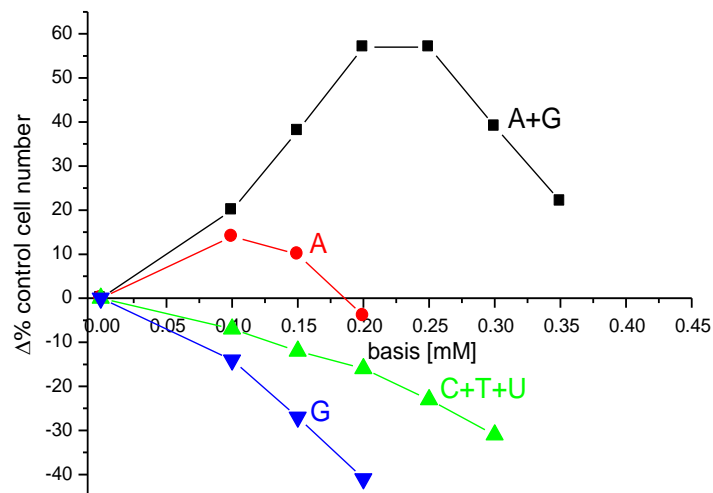
Fig. 16. The effect of the somministration of purine (A=Adenine, G=Guanine) and pyrimidine (C=Citosine, T=Thymidine, U=Uracile) bases on the proliferation of K562 cells treated with Antimycin A. The values reported here are means ± SEM of three independent measurements.

The above indications should be reconciled with the fact that folate addition is equally necessary to remove the blockage of cell recruitment produced by the deficit of the mitochondrial respiration reported in this work (see above). We explained this fact recalling that purines synthesis relies on the NADP-dependent oxidation of methylen-FH_4 (CH_2FH_4) to methenyl-FH_4 (CH_4FH_4) operated by methylen-FH_4 dehydrogenase. This NADP-dependent reaction, not required for pyrimidine synthesis, is evidently regulated by the NADPH/NADP ratio.

As shown in Fig.17, this ratio is strongly enhanced when the mitochondrial respiration is impaired by Antimycin A. This enhancement makes it obviously difficult or impossible the NADP-dependent conversion of CH_2-FH_4 to CH-FH_4.
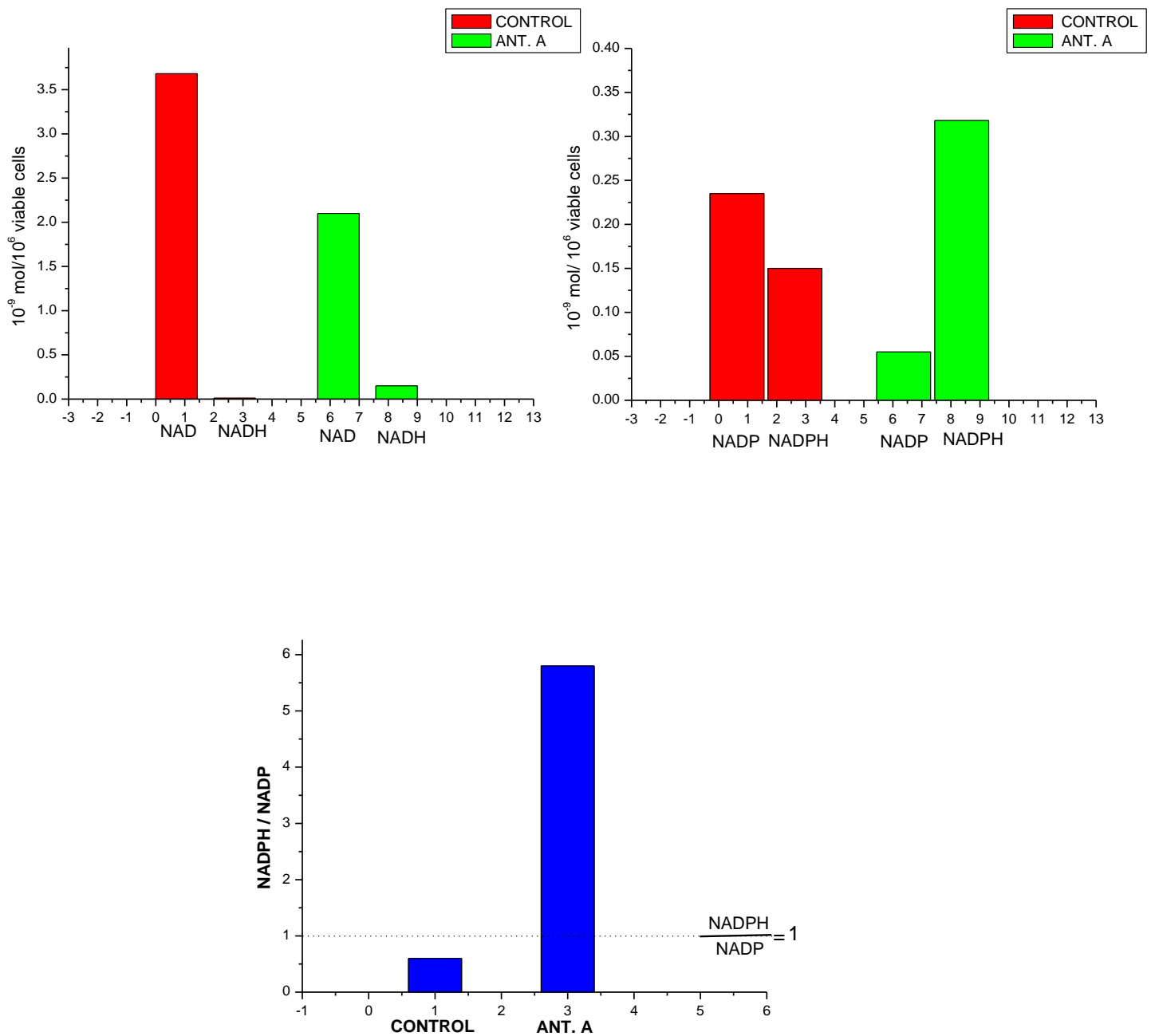
**Fig. 17. NAD, NADH, NADP and NADPH dosages and ratios in K562 cells in normoxia or in Antimycin A.** The nucleotides were measured by HPLC as reported in Materials and Methods.

To conclude, the experiments reported so far indicate that the enhancement of NADPH/NADP ratio is the eventual metabolic event that triggers the blockage of cell recruitment to S produced by the impairment of the respiratory chain under hypoxic conditions.

The inhibition of K562 cell recruitment into the cycling state by pyruvate

The results presented so far point out a strong similarity of the metabolic mechanism underlying the hypoxia-dependent cell growth arrest of K562 as compared to that of Yoshida cells (see above). In the case of ascites cells this mechanism resulted to be produced not only by the block of electron transfer of reducing equivalents to O_2 (N_2 atmosphere, Antimycin A) but also by the saturation of the chain by the preferential oxidation of physiological substrates, chiefly pyruvate. To check whether this latter metabolic feature is also displayed by K562 cells, we measured the effect of pyruvate on K562 growth. As shown in Fig. 18, pyruvate indeed inhibits K562 cell growth although at doses about 2-fold higher than those effecting the AH130 growth.
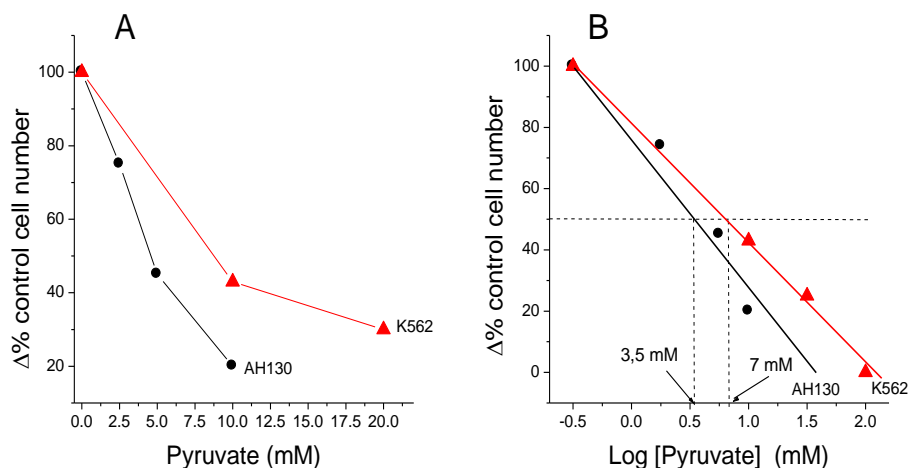
Fig. 18. The cell growth inhibition by pyruvate on AH130 (black) and K562 (red) cells.
The values reported here are means ± SEM of three separate experiments for each cell line.

CONCLUDING REMARKS

Although carried out in two far different experimental systems, (AH130 ascites hepatoma and the K562 leukaemia), the crucial messages emerged are essentially the same.

Briefly, the Yoshida model led to establish the following points:

1) cell transition from the non-cycling to the cycling state strictly depends on the activity of the mitochondrial respiratory chain, even when the overall energy requirements of the cells can be supplied exclusively by the glycolytic ATP (see Introduction-Table 1B). The fundamental role of respiration is to exploit the reoxidation of reducing equivalents (electrons) deriving from some oxidative step connected with purine biosynthesis;

2) when added in excess, oxidizible substrates, chiefly pyruvate and oxalacetate, mimic the effects of Antimycin A and N_2 incubation, producing a blockage of cell recruitment reversible upon addition of adenine;

3) the above effects of Antimycin A and N_2 are removed also by folate, suggesting that the respiration-dependent limiting step of the G1-S transition is framed within the folate metabolism.

As to point 2), we proposed that the inhibitory effects of oxidizable substrates in G1-S transition is due to a saturation of the respiratory chain, with the consequent enhancement of the overall cellular NAD(P)H/NAD(P) ratio. A similar sequence has been described by Williamson and Jones, after pyruvate addition to intact heart cells and mitochondria (Williamson and Jones, 1964). This enhancement in turn retards or impairs the oxidation of other substrates to

an extent depending on the sensitivities of the related dehydrogenases to variations of this ratio. In this light, the crucial process altered by pyruvate in our system is expected to be a NAD(P)-dependent step of purine (adenine) synthesis, leading to -the metabolic scheme reported below (Fig.19)
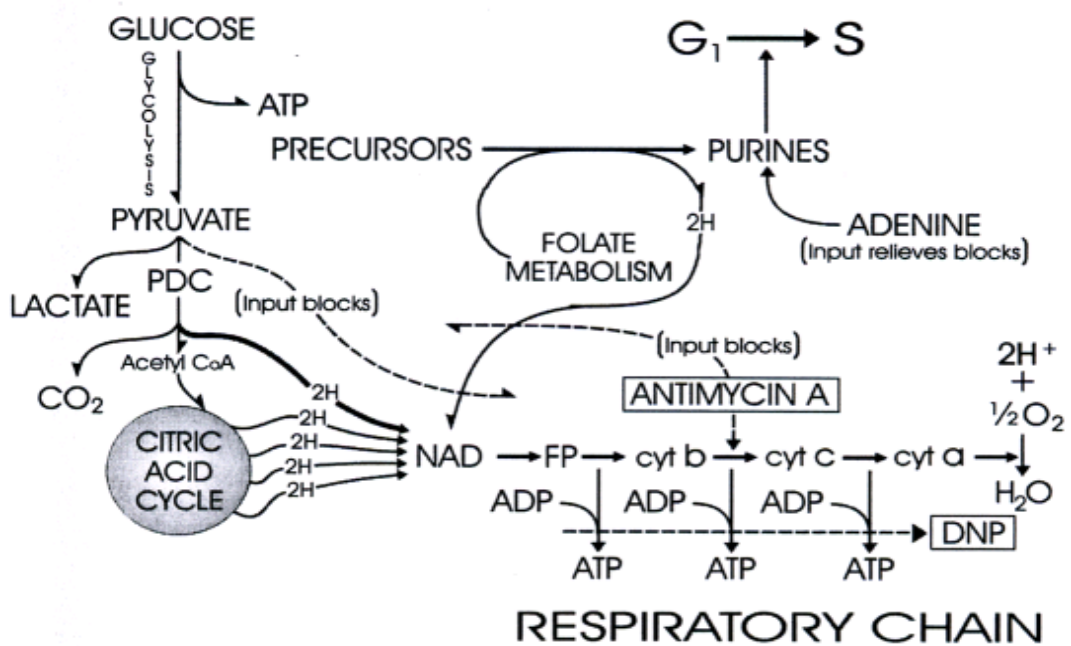
Fig. 19. Diagram indicating the redox mechanism controlling the stem cell transition from the non cycling to the cycling state. PDC=pyruvate dehydrogenase complex; FP=Flavoproteins; cyt=cytochrome (Olivotto and Dello Sbarba, 2008).

An accurate survey of the interplay of purine and folate metabolism with the cellular redox state is illustrated in the diagram reported below (Fig. 20)
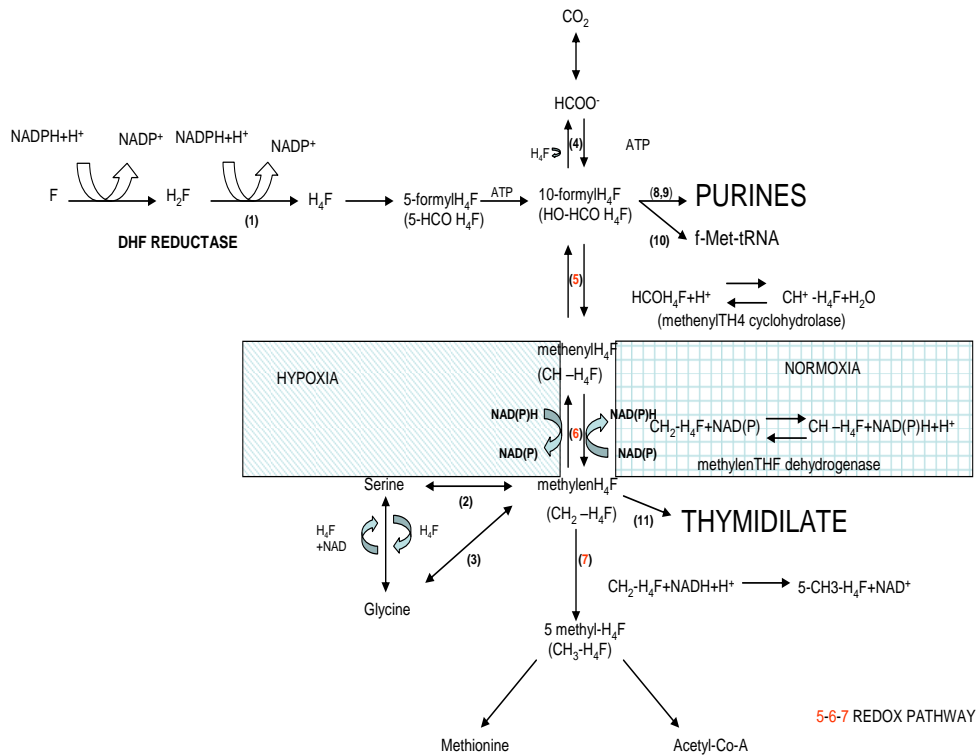
Fig. 20. Purine, Thymidilate and Folate Metabolic Pathway.

In mammals, the key reaction of the biosynthesis of purine and pyrimidine starts from methylen-FH_4 (CH_2FH_4). Noteworthy, the utilization of this compound is open to one or the other of the following options:

a) the direct utilization for the synthesis of thymidylate and hence of pyrimidine bases

b) the utilization for the synthesis of purine bases through the NADP–dependent oxidation to methenyl-FH$_4$ (CH-FH$_4$) catalyzed by the enzyme methylen-FH$_4$ dehydrogenase. This enzyme uses NADP as coenzyme in the so-called "central superhighway" of C$_1$ metabolism and FH$_4$ metabolism (Maden, 2000). The conversion of methenyl-FH$_4$ to 10-formyl-FH$_4$ (Reactions 5 and 6) in Fig. 20 are potentially reversible; however, in vertebrates they act together in the oxidative direction to provide 10-formyl-FH$_4$ which is the essential factor needed for the synthesis of the purine ring (reactions 8-9). Thus, in vertebrates, the metabolic pathway of purine synthesis requires a sufficiently low NADPH/NADP ratio to accomplish the C$_1$ "redox pathway".

In conclusion, since thymidilate synthesis is NADP-independent, when the NADPH/NADP ratio is high enough to hinder the NADP-dependent step of purine synthesis, the shift of the overall redox state produced by hypoxia or Antimycin A causes a substantial imbalance of the purine/pyrimidine equilibrium. This imbalance is entitled to produce DNA mutations unless the cell stops in G$_1$ or arrests in the first S phase. (Quéméneur *et al.*, 2003)

We consider not a pure chance the similarity of the metabolic profile of AH130 cells as compared to that of K562 cells. As a matter of fact, this similarity is high despite the high histogenetical distance of these two populations. The K562 hypoxic arrest of the cell cycle, as that of Yoshida cells, is based on a deficit of purine biosynthesis, which can be overcome by the addition of preformed purines and/or folate derivatives. Here again one is forced to admit a mechanism relying on a redox step connecting this synthesis with the NADP-

dependent step of CH_2FH_4 oxidation. However, a relevant difference consists in the fact that, this cycle arrest of K562 cells implies a cell accumulation in the S phase instead of in G1.

The arrest in G1 of Yoshida cells, as well as the arrest in S of K562 cells, can be explained by recalling that cells need to enlarge their purine bases before they are allowed to enter the phase of mitosis. We have shown that in AH130 cells do not express p53 protein and we've reconfirmed literature data (Lübert *et al.*,1988; Miyachi *et al.*,1999) according to the expression of this tumour suppressor is also abolished in the K562 cell line (Fig.9). So, although the cycle arrest in these two types of cells takes place in two different checkpoints, this blockage is caused in a p53-independent manner both in AH130 and in K562 cells.

A relevant point which deserves some further comments concerns the fact that pyruvate is a powerful tool to induce the cell cycle arrest in both types of cells. Indeed, in view of the cytostatic properties of this substrate, the essential feature of aerobic glycolysis, appears as a propitious feature for growth, as that is not affected by lactate accumulation in the medium without negative effects (Olivotto *et al.*, 1983). Consistently, anytime the oxidative capacity of the cells undergoes a severe limitation, the pyruvate-lactate conversion turns out to be decisive to allow a high glucose breakdown without creating the growth impairment which would result from pyruvate oxidation through the TCA. This metabolic device is essential to permit cell replication whenever the respiratory chain must be available for the oxidative step connected to purine metabolism or other essential pathways.

The above interpretation of our results is a profound revisitation of Warburg's theory and leads to propose that the "aerobic glycolysis" indeed

provides select advantage for tumour survival in restricted microenvironnement. In this light this cancer peculiarity should be taken into consideration when dealing with anaplastic tumour characterized by high rates of glycolysis and scarce oxidative capacity.

Finally, it is worth recalling that pyruvate brings about its cytostatic effects also in normal cells endowed with a scarce number of mitochondria such as normal hematopoietic progenitors and lymphocytes, suggesting that the profile emerged in this work is a general metabolic asset as in all type of stem cells destined to survive for indefinite time in a quiescent state.

BIBLIOGRAPHY

Baird SM. Hematopoietic stem cells in leukemia and lymphoma. In*: Sell S, editor: Stem Cells Handbook. Totowa, Humana Press, 2003, pp 163-175.*

Bartram CR, de Klein A, Hagemeijer A, van Agthoven T, Geurts van Kessel A, Bootsma D, Grosveld G, Ferguson-Smith MA, Davies T, Stone M, *et al.* Translocation of c-ab1 oncogene correlates with the presence of a Philadelphia chromosome in chronic myelocytic leukaemia. *Nature. 1983 Nov 17-23;306(5940):277-80.*

Bjerkvig R, Tysnes BB, Aboody KS, Najbauer J, Terzis AJ. Opinion: the origin of the cancer stem cell: current controversies and new insights. *Nat Rev Cancer. 2005 Nov;5(11):899-904.*

Blagosklonny MV. Oncogenic resistance to growth-limiting conditions. *Nat Rev Cancer. 2002 Mar;2(3):221-5.*

Botwood N, James R, Vernon C, Price P. Raltitrexed ('Tomudex') and radiotherapy can be combined as postoperative treatment for rectal cancer. *Ann Oncol. 2000 Aug;11(8):1023-8.*

Bruce WR, Van Der Gaag H. A quantitative assay for the number of murine lymphoma cells capable of proliferation in vivo. *Nature 1963;199:79–80.*

Bucher T., Czok R., Lamprecht W., Latzko E. Pyruvate. *1963; Methods in Enzymatic Analysis. H.U. Bergmeyer, ed. Academic Press, New York, pp.253-259.*

Chance B, Williams GR. The respiratory chain and oxidative phosphorylation. *Adv Enzymol 1956; 17:65-134.*

Cipolleschi MG, Dello Sbarba P, Olivotto M. The role of hypoxia in the maintenance of hematopoietic stem cells. *Blood.1993 Oct 1;82(7):2031-7.*

Cunningham D. Mature results from three large controlled studies with raltitrexed ('Tomudex'). *Br J Cancer. 1998;77 Suppl 2:15-21.*

Deininger MW, Goldman JM, Melo JV. The molecular biology of chronic myeloid leukemia. *Blood. 2000 Nov 15;96(10):3343-56.*

Del Monte U, Rossi CB. Glucose supply by the living host and glycolysis of Yoshida ascites hepatoma in vivo. *Cancer Res. 1963 Mar;23:363-7.*

Del Monte U. Changes in oxygen tension in Yoshida ascites hepatoma during growth. *Proc Soc Exp Biol Med. 1967 Jul;125(3):853-6.*

Dello Sbarba P, Cipolleschi MG, Olivotto M. Hemopoietic progenitor cells are sensitive to the cytostatic effect of pyruvate. *Exp Hematol. 1987 Feb;15(2):137-42.*

Fidler IJ. Tumor heterogeneity and the biology of cancer invasion and metastasis. *Cancer Res. 1978 Sep;38(9):2651-60.*

Folkman J. What is the evidence that tumors are angiogenesis dependent? *J Natl Cancer Inst. 1990 Jan 3;82(1):4-6.*

Furth, J. & Kahn, M. C. The transmission of leukaemia of mice with a single cell. Am J. Cancer *31, 276–282 (1937).*

Groffen J, Stephenson JR, Heisterkamp N, de Klein A, Bartram CR, Grosveld G. Philadelphia chromosomal breakpoints are clustered within a limited region, bcr, on chromosome 22. *Cell. 1984 Jan;36(1):93-9.*

Hamburger AW, Salmon SE. Primary bioassay of human tumor stem cells. *Science 1977;197:461–3.*

Hohorst, H.J. L(+)Lactate determination with lactate dehydrogenase and DPN. *(1963) Methods in Enzymatic Analysis. H.U. Bergmeyer, ed. Academic Press, New*

York, pp.266-270.

Jones RJ, Matsui WH, Smith BD. Cancer stem cells: are we missing the target? *J Natl Cancer Inst. 2004 Apr 21;96(8):583-5.*

Jordan CT, Guzman ML, Noble M..,Cancer stem cells. *N Engl J Med. 2006 Sep 21;355(12):1253-61.*

Jørgensen HG, Holyoake TL. Characterization of cancer stem cells in chronic myeloid leukaemia. *Biochem Soc Trans. 2007 Nov;35(Pt 5):1347-51.*

Klein CA. The systemic progression of human cancer: a focus on the individual disseminated cancer cell--the unit of selection. *Adv Cancer Res. 2003;89:35-67.*

Klein G. Foulds' dangerous idea revisited: the multistep development of tumors 40 years later. *Adv Cancer Res. 1998;72:1-23.*

Konopleva M, Tabe Y, Zeng Z, Andreeff M. Therapeutic targeting of microenvironmental interactions in leukemia: mechanisms and approaches. *Drug Resist Updat. 2009 Aug-Oct;12(4-5):103-13.*

Lardy HA, Wellmann H. Oxidative phosphorylation. Role of inorganic phosphate and acceptor system in control of metabolic rates. *J Biol Chem 1952; 195: 215-24*

Lemoli RM, Bertolini F, Cancedda R, De Luca M, Del Santo A, Ferrari G, Ferrari S, Martino G, Mavilio F, Tura S. Stem cell plasticity: time for a reappraisal? *Haematologica. 2005 Mar;90(3):360-81.*

Loeb LA. Cancer cells exhibit a mutator phenotype. *Adv Cancer Res. 1998;72:25-56.*

Loeb LA, Cheng KC. Errors in DNA synthesis: a source of spontaneous mutations. *Mutat Res. 1990 May;238(3):297-304.*

Loomis WF, Lippmann F. Reversible inhibition of the coupling of phosphorylation and oxidation. *J Biol Chem 1948; 173:807-8.*

Lübbert M, Miller CW, Crawford L, Koeffler HP. p53 in chronic myelogenous leukemia. Study of mechanisms of differential expression. *J Exp Med. 1988 Mar 1;167(3):873-86.*

Lu X, Errington J, Chen VJ, Curtin NJ, Boddy AV, Newell DR. Cellular ATP depletion by LY309887 as a predictor of growth inhibition in human tumor cell lines. *Clin Cancer Res. 2000 Jan;6(1):271-7.*

Maden BE. Tetrahydrofolate and tetrahydromethanopterin compared: functionally distinct carriers in C1 metabolism. *Biochem J. 2000 Sep 15;350 Pt 3:609-29. Review.*

Makino S, Kano K. Cytological studies of tumors. XIV. Isolation of single-cell clones from a mixed-cell tumor of the rat. *J Natl Cancer Inst. 1955 Apr;15(5):1165-81.*

Merlo LM, Pepper JW, Reid BJ, Maley CC. Cancer as an evolutionary and ecological process. *Nat Rev Cancer. 2006 Dec;6(12):924-35.*

Mittal S, Mifflin R, Powell DW. Cancer Stem Cells: The Other Face of Janus. *Am J Med Sci 2009;338(2):107–112.*

Miyachi T, Adachi M, Hinoda Y, Imai K. Butyrate augments interferon-a-induced S phase accumulation and persistent tyrosine phosphorylation of cdc2 in K562 cells. *British Journal of Cancer(1999) 79(7/8), 1018–1024.*

Mughal TI, Goldman JM. Chronic myeloid leukemia: why does it evolve from chronic phase to blast transformation? *Front Biosci. 2006 Jan 1;11:198-208.*

National Cancer Institute, 2008.
http://www.meb.unibonn.de/cancer.gov/CDR0000258001.html

Nelson DL, Cox MM. I principi di biochimica di Lehninger. *Zanichelli, third edition 2002, 15:517-35.*

Nowell PC. The clonal evolution of tumor cell populations. *Science. 1976 Oct 1;194(4260):23-8.*

Nowell, P., Hungerford, D. A minute chromosome in human chronic granulocytic leukemia. *Science. 1960; 132:1497-1501.*

Olivotto M and Dello Sbarba P. Environmental restrictions within tumor ecosystems select for a convergent, hypoxia-resistant phenotype of cancer stem cells. *Cell Cycle. 2008 Jan 15;7(2):176-87.*

Olivotto M, Arcangeli A, Caldini R, Chevanne M, Cipolleschi MG, Dello Sbarba P. Metabolic aspects of cell cycle regulation in normal and cancer cells. *Toxicol Pathol. 1984;12(4):369-73.*

Olivotto M, Caldini R, Chevanne M, Cipolleschi MG. The respiration-linked limiting step of tumor cell transition from the non-cycling to the cycling state: its inhibition by oxidizable substrates and its relationships to purine metabolism. *J Cell Physiol. 1983 Aug;116(2):149-58.*

Olivotto M, Dello Sbarba P, Cipolleschi MG. Hypoxia as a determining factor in the maintenance of stem cell function in the bone marrow haemopoietic tissue. *Blood Transf 2003; Blood Transf 2003; 2: 118-26.*

Olivotto M, Paoletti F. Studies on the kinetics of initial cycle progression in vitro of ascites tumour cells subsequent to isolation from ascites fluid. *Cell Tissue Kinet. 1980 Nov;13(6):605-12.*

Olivotto M, Paoletti F. The role of respiration in tumor cell transition from the noncycling to the cycling state. *J Cell Physiol. 1981 May;107(2):243-9.*

Olivotto M. Cytokinetic and metabolic studies on transition of tumour cells and lectin-stimulated lymphocytes from the non cycling to the cycling state. *Professorship Thesis, STIAV Publisher, Firenze, Italy, 1979; 1-36.*

Paget S. The distribution of secondary growths in cancer of the breast. *Lancet 1889, 1:571-572.*

Pardal R, Clarke MF, Morrison SJ. Applying the principles of stem-cell biology to cancer. *Nat Rev Cancer. 2003 Dec;3(12):895-902*.

Park CH, Bergsagel DE, McCulloch EA. Mouse myeloma tumor stem cells: a primary cell culture assay. *J Natl Cancer Inst 1971;46:411–22.*

Quéméneur L, Gerland LM, Flacher M, Ffrench M, Revillard JP, Genestier L. Differential control of cell cycle, proliferation, and survival of primary T lymphocytes by purine and pyrimidine nucleotides. *J Immunol. 2003 May 15;170(10):4986-95.*

Quesenberry PJ, Colvin GA, Lambert JF. The chiaroscuro stem cell: a unified stem cell theory. *Blood. 2002 Dec 15;100(13):4266-71.*

Ramaiah E. Pasteur effect and phosphor fructokinase. In current topic in cellular regulation. *1974; Horecker BL and Standmann ER Eds; Academic Press, New York 8: 297-345.*

Rous P, Beard JW. The progression to carcinoma of virus-induced rabbit papillomas. *J Exp Med. 1935 Sep 30;62(4):523-548.*

Rowley JD. Letter: A new consistent chromosomal abnormality in chronic myelogenous leukaemia identified by quinacrine fluorescence and Giemsa staining. *Nature. 1973 Jun 1;243(5405):290-3.*

Rowley JD. The role of chromosome translocations in leukemogenesis. *Semin Hematol. 1999 Oct;36(4 Suppl 7):59-72.*

Sawyers CL. Chronic myeloid leukemia. *N Engl J Med. 1999 Apr 29;340(17):1330-40.*

Schmidt CA, Przybylski GK. What can we learn from leukemia as for the process of lineage commitment in hematopoiesis? *Int Rev Immunol. 2001 Feb;20(1):107-15.*

Sell S. Stem cell origin of cancer and differentiation therapy. *Crit Rev Oncol Hematol. 2004 Jul;51(1):1-28.*

Stemline.com, 2008

Van Cutsem E, Cunningham D, Maroun J, Cervantes A, Glimelius B. Raltitrexed: current clinical status and future directions. *Ann Oncol. 2002 Apr;13(4):513-22.*

Vaupel P, Harrison L. Tumor hypoxia: causative factors, compensatory mechanisms, and cellular response. *Oncologist. 2004;9 Suppl 5:4-9.*

Vaupel P, Kallinowski F, Okunieff P. Blood flow, oxygen and nutrient supply, and metabolic microenvironment of human tumors: a review. *Cancer Res. 1989 Dec 1;49(23):6449-65.*

Vaupel P. The role of hypoxia-induced factors in tumor progression. *Oncologist. 2004;9 Suppl 5:10-7.*

Warburg O. On respiratory impairment in cancer cells. *Science 1956; 124: 269-70.*

Warburg O. On the origin of cancer cells. *Science 1956; 123:309-14.*

Warburg O. The metabolism of tumours. *Constable, London, 1959.*

Werner W., Rey H.G., Wielinger H. Über die Eigenschaften eines chromogenes für die Blutzuckerbestimmung nach der GOD/POD-Methode. *1970; Z .Anal.Chem., 252: 224-228.*

Williamson J.R. and Jones E.A. Inhibition of glycolysis by pyruvate in relation to the accumulation of citric acid cycle intermediates in the perfused rat heart. *1964; Nature, 203: 1171-1173.*

Yoshida T. Experimental production of tumours by subcutaneous injection of an olive oil solution of o-aminoazotoluene.*. Gann. 1934b; 28, 441.*

THANKS

First of all, I would like to thank Prof. Massimo Olivotto for giving me the opportunity to dedicate myself to the thing I love the most that is, Oncology Research. I'd like to thank him for believing in my capacities as a young researcher and for making me believe in my researcher potentials. I'm grateful to him for all the things that he has taught me about research but also for our long talks about politics, religion, art and his beloved city, Florence-a city that nowadays I adore as well. I thank him for remembering me that in this world, they do exist people successful in their scientific work but in contemporary with a great culture about art and most importantly with a great humanity and kindness. I'd like to thank Prof. Olivotto for showing me that truly superior people are characterized by a sincere humility.

A great thanks to Dot.ssa Maria Grazia Cipolleschi for all her research teaching but also for her maternal affect and encouragement. I'd also to thank all my lab colleagues: David, alias Dino, for all the friendship, help and support that he gave to me during these three years *(… e se pensiamo che grazie anche a te sono venuta a fare il dottorato da voi),* Ilaria for all the advices and support during our daily job, Massimo for all the help that he gave me during my research but also for our conversations about music or everyday events -*Massimì la greca ti ringrazia*!!!

I would like to thank Prof. Persio Dello Sbarba for all the kindness, warmth and helpfulness he showed me. I allow myself to that say he is a really worth follower of his maestro, Prof.Olivotto-he really enforces "the extraordinary force of gentleness".

I would like to express my thankfulness to all my colleagues of Prof. Dello Sbarba's laboratory: Serena, Valentina, Andrea, Michele, Elisabetta, Silvia for all the friendship that showed me and for all the help and advices that gave to me during my work. I would also like to thank my colleague Matteo but also Marco, Stefano and Walter for all their helpfulness and kindness.

A great thanks to my dear friends Lucia, Raffaele, Manuela, Susanna, Ussy, Andrea and Yasemin for all the friendship and affection that have given to me and for making these three years in Florence unforgettable. Thank you for all the conversations that we've had, for all the Saturday "casa Raffy" and Sunday "pizzetta da Dora" dinners, for all our dancing nights, for all our "festa-festa," for all the dawns that we've lived together, for all the concerts that we've been together, for all

the walks in the center of Florence, for all our excursions outside the city. I'm so thankful for finding friends like you with whom I can share my interests and who have become my family here in Florence and will continue to be even when (or if – you never know) I leave Italy. Thank you for all the love that you give to me and for all the love that you make me feel.

I would like also to thank George for showing me how vital is to listen to yourself and to live your real passions and dreams.

I would like to thank my precious friends Josephine, Lina, Christianna, Dimitris, Nasos, Thanos, Thanasis, Ada, Yanni, Nikos, Ada for all their support. Thanks to them I've never felt alone here in Italy. During all these years that I've lived in Tuscany, they have made me feel that they are always next to me even in the hardest, darkest moments that I spent away from my beloved Athens.

Above all, I would like to thank Yianna, my mother, the finest, strongest woman I know to whom I owe everything. Without her, I wouldn't have studied Oncology and I wouldn't have all those principles and ideals she's given to me for which I'm proud of no matter how hard they are to follow.

Thank you mum for everything, I love you.

Σ'ευχαριστώ μαμά για όλα, σ'αγαπώ.